

NIS CATHODE FOR GCAP SYSTEM FOR USE IN CONCENTRATED H<sub>2</sub>SO<sub>4</sub>

FEASIBILITY OF NICKEL SULPHIDE AS A CATHODE IN A GALVANIC  
COUPLED ANODIC PROTECTION SYSTEM FOR USE IN  
CONCENTRATED SULPHURIC ACID SYSTEMS

By: ANIRUDDHO PAL, B. Eng

A Thesis Submitted to the School of Graduate Studies in Partial Fulfilment of the  
Requirements for the Degree Master of Applied Science

McMaster University © Copyright by Aniruddho Pal, April 2013

McMaster University MASTER OF APPLIED SCIENCE (2012) Hamilton,  
Ontario (Engineering)

TITLE: Feasibility of Nickel Sulphide as a cathode in a Galvanic Coupled Anodic  
Protection System for use in Concentrated Sulphuric Acid Systems AUTHOR:  
Aniruddho Pal, B. Eng. (McMaster University) SUPERVISOR: Dr. J.R. Kish and  
Dr. N. Provatas NUMBER OF PAGES: ix, 101

## Abstract

Anodic protection has shown to be a viable method for reducing corrosion rates of stainless steels over a wide range of temperatures and is used to protect equipment in H<sub>2</sub>SO<sub>4</sub> manufacturing. While effective at controlling corrosion in H<sub>2</sub>SO<sub>4</sub> manufacturing, Impressed Current Anodic Protection (ICAP) systems have shown to have a number of issues. They require a constant source of current to ensure reliable corrosion protection; are relatively complex systems and expensive to install; improper potential control can lead to loss of corrosion protection; and some issues with cathode fouling and erosion have been reported. Galvanic Coupled Anodic Protection (GCAP) systems have not been widely utilized in industry, but offer some solutions to these issues. GCAP systems have been developed using Pt and Au as the cathode materials for use in H<sub>2</sub>SO<sub>4</sub>. Previous work on the oscillatory behaviour of austenitic stainless steels indicates that nickel sulphide (NiS) could be used as cathode material in a GCAP system in concentrated H<sub>2</sub>SO<sub>4</sub> to protect stainless steel. The objective of this study was to develop a better understanding of the behaviour of NiS when galvanically coupled to Type 430 stainless steel to determine whether it can be used in a GCAP system. NiS and NiS(Ni) electrodes are able to provide the  $I_{crit}$  needed to passivate Type 430 at anode/cathode ratios of 10:1, while NiS(Ni) electrodes were able to provide the  $I_{crit}$  needed to passivate the Type 430 stainless steel at a ratio of 20:1. In addition it was shown that the NiS(Ni) electrode was able to maintain passivity of the Type 430 stainless steel array using an anode/cathode surface area ratio of 100:1. NiS was shown not to be inert in concentrated H<sub>2</sub>SO<sub>4</sub> and corrosion rate calculated via Tafel extrapolation and shown to be 0.014 mm/yr at room temperature and 0.128 mm/yr at 60 °C.

## **Acknowledgments**

I would like to express my deepest gratitude to my academic supervisors, Dr. J.R. Kish and Dr. N. Provatas, for their guidance, encouragement and insight throughout my research. Their help and support during my research was beyond what I could have asked for, and for this I sincerely thank them.

My co-workers at the Walter W. Smeltzer Corrosion Laboratory, McMaster University, deserve my thanks as well. Their comradery and support made my time working with them truly enjoyable and an experience I will soon not forget. Special thanks must be given to Stephen Jones for his immense expertise and help while conducting research in concentrated sulphuric acid. Many hours were spent in the acid lab conducting and discussing our research, and his insight and help was critical to this research. I would also like to thank Jacek Dabrowski for his friendship and support during some trying times.

I would like to thank the following people for their technical expertise in helping further my research. Jim Garrett from the Brockhouse Institute for Materials Research, McMaster University, for synthesizing the NiS sample used in my experiments. Jim Britten from the McMaster Analytical X-ray Diffraction Facility, McMaster University, for helping characterize the NiS sample. Doug Culley from the Materials Engineering Lab for his help with GDOES analysis.

Lastly, I cannot adequately express the my gratitude to my family. Their love, encouragement and support during my career as a student through all the ups and downs has truly been a blessing, and for that I am eternally grateful.

## Table of Contents

Table of Contents.....	vi
List of Figures and Tables.....	viii
Introduction .....	1
Literature Review.....	7
Passivity.....	8
Properties of H <sub>2</sub> SO <sub>4</sub> - H <sub>2</sub> O Systems.....	17
Physical and Chemical Properties.....	17
Electrochemical Properties.....	20
Anodic Protection.....	23
Impressed Current Anodic Protection (ICAP).....	24
Galvanic Couple Anodic Protection (GCAP).....	39
Galvanic Effect in Metal Sulphides.....	38
Summary.....	41
Experimental Details.....	43
Materials and Solution .....	43
Metals.....	43
Nickel Sulphide.....	44
Solution.....	47
Electrode Preparation .....	47
Mounted Electrodes.....	47
Suspended Electrodes.....	48
NiS Electrode .....	50
Electrochemical Tests.....	50
Open Circuit Potential Measurements.....	50
Polarization Measurements.....	51
Galvanic Couple Tests.....	52
Surface Area Relationship: NiS – Type 430.....	52

Surface Area Relationship: NiS(Ni) – Type 430.....	53
Shielding Experiments.....	54
Results.....	57
Polarization Experiments.....	57
Cathodic Polarizations.....	57
Anodic Polarization.....	62
Galvanic Couple Experiments.....	63
NiS Surface Area Relationships.....	63
NiS(Ni) Surface Area Relationships.....	67
Shielding Experiments.....	71
Discussion.....	78
Ability to Initiate Passivity.....	79
Surface Area Ratios.....	82
Maintaining Passivity .....	86
Transpassivation .....	90
Overall Circuit Resistance.....	91
Summary.....	92
Conclusion and Future work.....	94
References.....	97

## List of Figures and Tables

Table 1: Physical properties of H <sub>2</sub> SO <sub>4</sub> and H <sub>2</sub> O [30-31].....	18
Table 2: Current density require to passivate and maintain passivity of a variety of alloys in different concentrations of sulphuric acid [5] .....	28
Table 3: Cathode materials used in ICAP systems for H <sub>2</sub> SO <sub>4</sub> applications [5,7-8] .....	29
Table 4: Electric Resistivities of a number of metal sulphides.....	40
Table 5: Rest potentials of some sulphide minerals [63].....	41
Table 6: Average composition of samples vs. standard composition of Type 430 .....	45
Table 7: Summary of GCAP systems and the surface area ratios needed for passivation.....	86
Figure 1: Anodic polarization of Ni in 5 M H <sub>2</sub> SO <sub>4</sub> showing passivation behaviour [4].....	10
Figure 2: Chemical composition of H <sub>2</sub> SO <sub>4</sub> -H <sub>2</sub> O solutions: a) Concentration of species [35] b) Concentration and structure of hydrated protons [36].....	19
Figure 3: Redox potential of H <sub>2</sub> SO <sub>4</sub> - H <sub>2</sub> O solutions at 25 °C. a) Banaś and Stypula [33] b) Sridhar [32].....	21
Figure 4: Potentiodynamic cathodic polarization of 93.5 wt% H <sub>2</sub> SO <sub>4</sub> measured on rotating platinum electrode (500 rpm) [9].....	22
Figure 5: Schematic of Ti coupled to Pt and Ni [47].....	32
Figure 6: Surface area ratios needed to passivate S30400 with platinum at a variety of temperatures and concentrations of sulphuric acid [47].....	34
Figure 7: Potential readings during Type 430 - NiS(Ni) couple experiment [9]....	36
Figure 8: Corrosion potential of nickel electrode as a function of time in 93.5 wt% H <sub>2</sub> SO <sub>4</sub> at 60 °C [9].....	37
Figure 9: a) XRD <sup>2</sup> analysis of NiS sample. b) Single crystal analysis of NiS	

Sample.....	46
Figure 10: Princeton Research K105 Flat Specimen holder® with a Kalrez® washer.....	48
Figure 11: Examples of suspended Type 430 electrodes; a) 75 cm <sup>2</sup> , b) 100 cm <sup>2</sup> ...	49
Figure 12: Examples of suspended NiS(Ni) electrodes; a) 47.3 cm <sup>2</sup> , b) 24 cm <sup>2</sup> c) 5cm <sup>2</sup> .....	49
Figure 13: Exposed Surface of NiS electrode.....	50
Figure 14: Galvanic couple surface area experiment.....	54
Figure 15: Schematic of coupon placement in HDPE tank.....	55
Figure 16: Cathodic polarizations of NiS at room temperature and 60°C.....	58
Figure 17: Cathodic polarization of NiS(Ni) at room temperature and 60 °C.....	59
Figure 18: Cathodic polarization of Pt at room temperature and 60 °C.....	61
Figure 19: Anodic polarization of Type 430 at room temperature and 60 °C.....	62
Figure 20: Evans diagram showing the possible galvanic potential of Type 430 : NiS surface area ratios.....	64
Figure 21: Potential on NiS and 430 surface during galvanic couple experiment; a) 10:1 (SS:NiS) ratio b) 100:1 (SS:NiS) ratio.....	65
Figure 22: Evans diagram showing the possible galvanic potential of both Type 430: NiS(Ni) surface area ratios.....	67
Figure 23: Potential on NiS and Type 430 surface during galvanic couple experiment; a) 10:1 (SS:NiS(Ni)) ratio b) 100:1 (SS:NiS(Ni)) ratio.....	69
Figure 24: Evans diagram showing the possible galvanic potential of three Type 430 : NiS(Ni) surface area ratios.....	72
Figure 25: Potentials on Stainless Steel coupons for 10:1 and 20:1 surface area ratios; (a) 1 h (b) 4 h (c)10 h (d) 24 h.....	75
Figure 26: Potentials of array when uncoupled, coupled to 100 to 1 and then 20 to 1 surface area ratios.....	76
Figure 27: Potential on Type 430 array when coupled to 100 to 1 surface area ratio	

.....	77
Figure 28: Evans diagram of polarization behaviour of cathode and anode materials at room temperature in quiet 93.5 wt% H <sub>2</sub> SO <sub>4</sub> .....	80
Figure 29: Evans diagram of polarization behaviour of cathode and anode materials 60 °C in quiet 93.5 wt% H <sub>2</sub> SO <sub>4</sub> .....	81
Figure 30: Determination of corrosion current densities of electrodes using Tafel extrapolation.....	88
Figure 31: Surface area ratios needed to maintain passivate Type 430 at room temperature.....	90
Figure 32: Comparison of anodic polarization behaviour of Type 430 and Type 304L in 93.5 wt% H <sub>2</sub> SO <sub>4</sub> at 60 °C [9].....	93

## **CHAPTER 1**

### **Introduction**

During the manufacturing process of commercial grade sulphuric acid (93 – 99 wt% H<sub>2</sub>SO<sub>4</sub>), the acid can reach temperatures of up to 120 °C [1]. Thus the choice of construction materials required in the manufacturing process is primarily dictated by the corrosion resistance at these relatively high process temperatures. Generally for pump tanks, piping and heat exchangers, Type 316L and Type 304L stainless steels have been used successfully to handle concentrated H<sub>2</sub>SO<sub>4</sub> [1-3]. However, Type 316L and Type 304L stainless steel both have limited corrosion resistance to concentrated H<sub>2</sub>SO<sub>4</sub> at elevated temperatures. At higher temperatures (above 75 °C), the passive film that protects the stainless steel can

periodically breakdown and the stainless steel corrodes rapidly during these periods [3]. For example, Type 316L stainless steel exposed to 93 wt% H<sub>2</sub>SO<sub>4</sub> at 100 °C has shown to corrode at rate of up to 12.6 mm/yr [2]. Anodic protection has shown to be a viable method for reducing corrosion rates of stainless steels over a wide range of temperatures including elevated process temperatures, for example reducing the corrosion rate of Type 316L stainless steel exposed to 93 wt % H<sub>2</sub>SO<sub>4</sub> at 100 °C from 12.6 mm/yr to 0.64 mm/yr [2].

Anodic protection is used to raise the potential on the surface of the stainless steel to a potential greater than the passivation potential ( $E_{pp}$ ) in order to stabilize and maintain the passive film. This is accomplished by either impressing an external anodic current [Impressed Current Anodic Protection (ICAP)] or by galvanically coupling the stainless steel to an appropriate more noble material [Galvanic Coupled Anodic Protection (GCAP)].

ICAP is the more commonly used protection method and has been used extensively in the H<sub>2</sub>SO<sub>4</sub> manufacturing industry in order to protect stainless steel piping and heat exchangers [1-4]. This type of protection system has a number of benefits, foremost being that corrosion rates are reduced when implemented properly. In addition, the maintenance costs of such a system are relatively low and manufacturing plants using anodic protection produce a higher purity acid with a lower iron content when compared those systems not using anodic

protection [1,4]. In fact, applications in H<sub>2</sub>SO<sub>4</sub> manufacturing account for the bulk of ICAP systems in use around the world today. However, there are also some significant issues associated with ICAP systems. ICAP systems are a three electrode system, where the protected stainless steel acts as the anode, the current is impressed through a counter electrode that acts as a cathode, and a reference electrode. The reference electrode is needed to monitor the potential of the anode and is an integral part of an ICAP systems. Such systems require a constant current to ensure reliable corrosion performance, as a loss of current could affect the integrity of the production system and damage the equipment, as it could lead to a breakdown of the protective passive film on the surface of the stainless steel, which would result in significantly higher corrosion rates. In addition, if the current applied is less than the critical current ( $I_{crit}$ ) needed to passivate or too low a potential is applied to the surface of the stainless steel, corrosion rates will increase significantly. In order to overcome the  $I_{crit}$ , the ICAP systems must be able to supply a large current and then maintain a much lower current in order to maintain the passive film. This requires large and expensive rectifiers and sophisticated reference electrodes, which monitor the potential on the surface of the stainless steel and work in a feedback loop with the rectifiers. Such equipment add to the cost and complexity of ICAP systems. If too high a potential is applied to the surface of the stainless steel, the stable passive film can breakdown, a

phenomena known as transpassivation, and can result in increased rates of corrosion. Lastly, problems with cathodes have been reported in ICAP systems used in  $\text{H}_2\text{SO}_4$  production including corrosion, erosion and fouling [7-8].

In principle, GCAP systems also help stabilize and maintain the protective passive films formed on stainless steel in corrosive media such as concentrated  $\text{H}_2\text{SO}_4$ . Such systems accomplish this by coupling the stainless steel, the anode, to an appropriate noble material, the cathode, which in turn reduces the corrosion rates of the stainless steel. This type of anodic protection system has not been used extensively in the  $\text{H}_2\text{SO}_4$  manufacturing industry, but offers some solutions to the problems encountered while using an ICAP system. While ICAP systems require a constant source of current to ensure reliable corrosion performance, GCAP systems are self passivating, if the correct anode to cathode surface area ratios are maintained. The current needed to protect the system is created via the electrochemical reactions occurring within the system, and, thus an external current is not needed. This reduces the complexity of the system considerably, since a power supply is not needed and reference electrodes are used only to monitor the system and work independently of the protection system. If a cathode material is picked such that its corrosion or redox potential is below that of the transpassivation potential of the stainless steel in the acid, then the threat of such a breakdown event can be eliminated and the reliability of such a system is

increased. Kish [9] studied the ability of nickel sulphide (NiS) grown in situ on a nickel substrate to protect non-nickel containing stainless steel, Type 430, in 93.5 wt% H<sub>2</sub>SO<sub>4</sub> when galvanically coupled and showed a reduction in the corrosion rate of the stainless steel by a factor of 120. Moreover, the corrosion potential of NiS is below that of the transpassivation of the stainless steel. Thus, NiS could be a viable material to use as a cathode in a GCAP systems for stainless steel in concentrated sulphuric acid.

The objective of this study is to develop a better understanding of the behaviour of NiS galvanically coupled to non-nickel containing stainless steels to determine whether it can be used in a GCAP system. The research objectives of this study are as follows:

1. To characterize the electroactive behaviour of monolithic NiS, and compare it to NiS grown in situ on nickel (NiS(Ni)).
2. To determine appropriate anode (stainless steel) to cathode (NiS) ratios that will induce galvanic passivation of the stainless steel.
3. To determine appropriate anode(stainless steel) to cathode (NiS) ratios that will maintain galvanic passivation of the stainless steel.

The feasibility of using a NiS electrode in a GCAP system is explored via a number of experiments to determine its ability to protect the non-nickel containing Type 430 stainless steel. Anodic and cathodic polarizations were

conducted on Type 430 stainless steel, NiS, NiS(Ni) and platinum to characterize their electrochemical behaviour in concentrated H<sub>2</sub>SO<sub>4</sub>. Surface area measurements were conducted to find the appropriate anode/cathode surface area relationships needed to initiate and maintain galvanic passivation. A set geometry was used to mimic a shell tube heat exchanger in order to test shielding effects, as well as the throwing power of the NiS(Ni) electrode. Experiments were conducted at both ambient temperatures and elevated temperatures to replicate processing temperatures. While most experiments were done with NiS grown in situ on a pure nickel substrate, a pure, monolithic NiS electrode was developed and tested as well.

## **CHAPTER 2**

### **Literature Review**

The concept of using NiS as a cathode material for a GCAP system to protect stainless steels in concentrated H<sub>2</sub>SO<sub>4</sub> was derived from research on the oscillatory potential behaviour of austenitic stainless steels [9-10]. A critical review of this research, as well as relevant literature in the fields of passivity, anodic protection and the properties of H<sub>2</sub>SO<sub>4</sub>-H<sub>2</sub>O solutions is presented. The review begins with a overview of metallic passivation behaviour, with particular attention given to passivation behaviour of austenitic stainless steels in H<sub>2</sub>SO<sub>4</sub>-H<sub>2</sub>O solutions. This is then followed by an investigation into the physical and electrochemical properties of concentrated H<sub>2</sub>SO<sub>4</sub> solutions. The properties of a

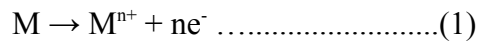
stainless steel – concentrated  $\text{H}_2\text{SO}_4$  system are examined and the use of anodic protection to protect such systems is analyzed. Industrial applications of ICAP systems are investigated and some of the shortcomings of these systems are highlighted. The theoretical background of GCAP systems is outlined and examples of such systems are analyzed. Lastly, the ability of metal sulphides, such as NiS, to form galvanic couples is investigated.

### **Passivity**

Passivity can be defined as a state of improved corrosion resistance resulting from the inhibition of the anodic process of metal dissolution despite a marked thermodynamic tendency to react [11]. Passivation occurs when certain materials, including stainless steels, form a thin, oxidized protective film on their surface in the presence of a corrosive environment, such as concentrated  $\text{H}_2\text{SO}_4$  which results in lower corrosion rates [4-5,11]. When stainless steels are placed in a corrosive solution, two electrochemical half cell processes occur on the metal surface, anodic (oxidation) and cathodic (reduction) half cell processes. Mixed potential theory [12-13] states that, in a given system the principle of charge conservation must be observed. Thus, the total sum of anodic oxidation current must equal the sum of cathodic reduction current in order to avoid accumulation of charge in the metal. In order to fulfill this requirement, both half cell processes are polarized from their equilibrium half-cell electrode potential to a common

potential,  $E_{\text{corr}}$ , and a common current,  $I_{\text{corr}}$ . When electrons are supplied to the electrode surface and there is an accumulation in the metal due to slow reaction rates, the surface potential becomes more negative and this is known as cathodic polarization. Anodic polarization occurs when electrons are removed from the metal and this causes a deficiency at the surface, thus making the surface potential more positive. Activation polarization is the potential change from the equilibrium half-cell electrode potential caused by a net surface reaction.

In stainless steel – concentrated  $\text{H}_2\text{SO}_4$  system, the generalized anodic reaction that occurs on the stainless steel is the oxidative metal dissolution reaction,



where M is the metallic atom (Fe,Cr,Ni,Mo) of the stainless steel,  $\text{M}^{n+}$  the cation of metal of n valence and  $\text{e}^-$  represents the electrons produced by the reaction. Metals and alloys that form oxidized protective films display a characteristic behaviour when anodically polarized as shown in Figure 1.

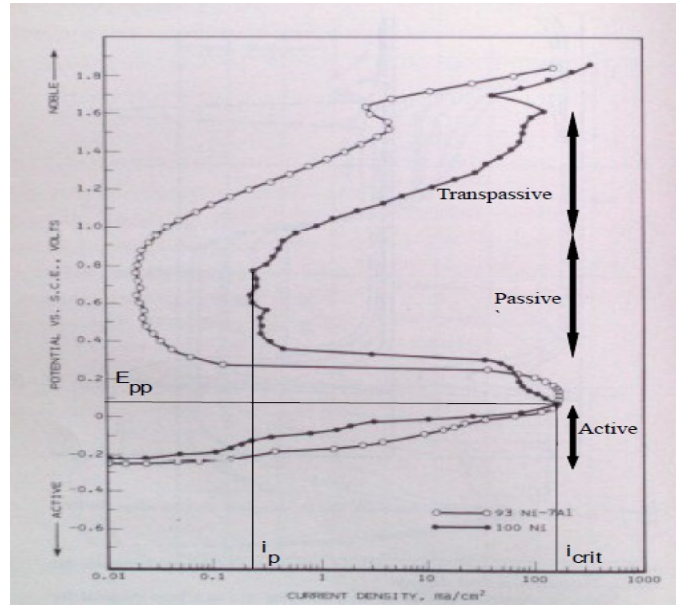


Figure 1: Anodic polarization of Ni in 5 M H<sub>2</sub>SO<sub>4</sub> showing passivation behaviour [4].

This behaviour is usually divided into three states; active, passive and transpassive. In the active state, increased activation polarization increases the dissolution reaction rate (anodic current density,  $i_a$ ). The anodic dissolution reaches a maximum and then decreases steeply with increasing anodic polarization. The associated potential at this maximum is known as the passivation potential ( $E_{pp}$ ) and the corresponding anodic current density is known as the critical current density ( $i_{crit}$ ). Beyond the  $E_{pp}$ , there is an inhibition of the anodic dissolution reaction, which corresponds to a sharp decrease in  $i_a$ . A thin, oxidized protective film begins to form on the surface of the metal above  $E_{pp}$  and corresponds to an inhibition of the anodic dissolution reaction and is known as the

active-passive transition. When the passive film has stabilized, a passive current density ( $i_p$ ) is established at positive potentials above  $E_{pp}$ , independent of potential. This current density is orders of magnitude lower than the  $i_{crit}$  and represents a significantly lower corrosion rate and is known as the passive state. At much higher potentials, the formed protective film breaks down or another mode of anodic dissolution begins, in which the oxidation valency of metal ions or oxygen ions increases and the anodic dissolution rate increases. This is known as the transpassive state.

The passivation behaviour shown in certain metals and alloys is due to the protective passive film formed on their surface when exposed to corrosive environments. Thus, it is important to understand the nature of these films. There has been extensive research done on this remarkable phenomena since it was defined by Keir in 1790 [14] especially on iron and ferrous alloys. The thickness, composition and structure of such protective films have been topics of extensive research. It is now generally accepted that passivity is caused by the presence of a thin, three-dimensional oxide film on the surface of the metal [15]. The composition of the passive film formed on iron and ferrous alloys is thought to involve one or more layers of oxides, hydroxides or oxyhydroxides [16]. Cahan and Chen [17] suggested that the chemical composition of the passive film on iron can be described as a highly protonated, trivalent iron oxyhydroxide capable of

existing over a relatively wide range of stoichiometry. Alloying elements such as chromium were introduced to improve the ability of iron to form a more protective passive film. The outer layer of the passive film of iron - chromium alloys is enriched with chromium and the film is made of a mixture of iron and chromium oxides, the chromium probably being a hydrated chromium oxyhydroxide [18]. Analytical studies show that the film is a duplex structure, consisting of an inner region composed of a few atomic layer of chromium oxide in contact with the metallic substrate and an outer region of iron oxides and hydroxides at the film – electrolyte interface [19]. While there is a general consensus as to the composition and structure of the passive film from on iron and stainless steel, the thickness and exact composition of the passive film can be altered by different factors, such as solution pH, chloride ions ( $\text{Cl}^-$ ) concentration, anodic aging time and the composition of the substrate on which is it formed [20-21].

Significant work has been done on the characterization of passive films formed on stainless steel in dilute  $\text{H}_2\text{SO}_4$ , using a variety of characterization techniques such as XPS and EIS [21-23,63]. The general agreement in literature is that the passivation of stainless steels in  $\text{H}_2\text{SO}_4$  is due to the formation of a  $\text{Cr}^{3+}$  compound and the enrichment of chromium in the passive film. XPS and EIS analysis of the major alloying components; chromium, iron and nickel, in stainless

steels, such as Types 316L, 216L and 304 yielded the following results [21-23,65]. Chromium was enriched in the passive layer, and oxidized in the passive film to form chromium oxide, with the top layer exposed to the solution mostly consisting of chromium hydroxide. Iron showed a lower concentration in the film than in the bulk, oxidizing to form oxides such as  $\text{Fe}_2\text{O}_3$ ,  $\text{FeO}$  as well as sulfites such as  $\text{FeS}$ ,  $\text{FeSO}_3$ , and  $\text{FeSO}_4$  in the passive layer. Nickel was enriched underneath the passive film and nickel compounds, such as  $\text{NiS}$  and  $\text{NiO}$ , were present in the passive layer. Examination of these studies lead to the conclusion that chromium and iron are preferentially oxidized in dilute  $\text{H}_2\text{SO}_4$  solutions in comparison to nickel and that the passive layer mainly is comprised of oxides, oxyhydroxides and sulfites of chromium and iron.

There is significantly less literature on the passive film composition of stainless steels when exposed to concentrated  $\text{H}_2\text{SO}_4$  solutions. However, some work has been conducted on pure iron, chromium and nickel. Mazurkiewicz [24] studied the anodic passive behaviour of iron at a variety of  $\text{H}_2\text{SO}_4$  concentrations using XPS. He found that the passive film formed on iron exposed to 18.8 M (100 wt%) is composed in its surface layer of hydroxides and oxides of  $\text{Fe}^{3+}$ , or  $\text{Fe}^{3+}$  and  $\text{Fe}^{2+}$ , with a certain hydration degree and small amounts of sulphates. The reduction of  $\text{Fe}^{3+}$  to  $\text{Fe}^{2+}$  and of  $\text{S}^{6+}$  to  $\text{S}^{2-}$  occurs in the bulk of the film and  $\text{H}_2\text{O}$  is also found in the bulk of the film.  $\text{FeO}$  oxides with  $\text{FeS}$  were found in contact

with the metal surface. Banaś et al. [25] analyzed the passive film formed on chromium in concentrated and anhydrous solutions of  $\text{H}_2\text{SO}_4$ . They found, using XPS analysis, that the passive film on chromium near the metal surface consisted mainly of oxide-hydroxide of  $\text{Cr}^{3+}$  with some  $\text{H}_2\text{O}$  molecules. In 18 M (98 wt%)  $\text{H}_2\text{SO}_4$ , the passive layer near the metal also contained an additional small amount of sulphate ions. A gradual dehydration in the layer was also observed. Zucchi et al. [63] studied the anodic behaviour of a range of Fe/Ni alloys including 99.5% Ni in concentrated  $\text{H}_2\text{SO}_4$  solutions. In 12.5 M (75 wt%)  $\text{H}_2\text{SO}_4$  solutions, a mixture of  $\text{FeSO}_4 \cdot \text{H}_2\text{O}$  and  $\beta\text{-NiSO}_4 \cdot 6\text{H}_2\text{O}$  were found on the surface of their samples. The iron compound was the predominant compound on the alloys with less than 50 wt% Ni while the  $\text{NiSO}_4$  was the more dominant compound on alloys having a greater than 50 wt% Ni. In 15 M (85 wt%)  $\text{H}_2\text{SO}_4$  solution, pure Ni was covered in a crystalline layer of  $\beta\text{-NiSO}_4 \cdot 6\text{H}_2\text{O}$  at all potentials up to  $+1.0 V_{\text{SCE}}$ . They determined that the anodic behaviour seemed to be influenced by the difference in the solubilities of the sulphates of Ni and Fe. They theorized that the  $\text{Fe}^{2+}$  ions that pass into the solution are precipitated to form a layer in which the  $\text{NiSO}_4$ , which does not precipitate on the pure metal, to form a layer at higher concentrations, remains embedded.

Kish and Li [9-10,26] studied the passive film formed on Type 304L when exposed to the 93.5 wt%  $\text{H}_2\text{SO}_4$  using AES, XPS and Laser Raman Spectroscopy.

Kish et al. [26] concluded that the anodic passivity involved the solid-state formation of a chromium rich oxide-hydroxide passive film with the participation of undissociated  $\text{H}_2\text{SO}_4$  as the source of oxygen. Nickel and sulphur ions were detected in the passive layer in both studies, which lead to the conclusion that nickel sulphide ( $\text{NiS}$ ) was formed in the passive layer of the Type 304L. Upon examination of these studies, they concluded that the passive films formed on stainless steels in concentrated  $\text{H}_2\text{SO}_4$  solutions is similar to those found in dilute  $\text{H}_2\text{SO}_4$  solutions, differing slightly in composition and thickness.

Nickel containing austenitic stainless steels have been found to exhibit spontaneous periodic active – passive potential oscillations when exposed to concentrated  $\text{H}_2\text{SO}_4$  and was first reported by Kain and Morris [27]. This behaviour has been studied extensively and a number of mechanistic models have been presented by Chang [28], Mitsuhashi et al. [29], Kish [9] and Li [10]. These studies theorized that the cause of the oscillations observed was the production of an intermediate corrosion product formed during active corrosion. This corrosion product was then able to able to passivate the stainless steel and maintain passivity till it was subsequently dissolved which caused re-activation. The composition of the corrosion product was disputed, Mitsuhashi and Chang [28-29] theorized it was  $\text{FeSO}_4$  with the production of sulphur playing a role. Kish and Li [9-10] theorized that the oscillations were caused by the formation of a  $\text{NiS}$

corrosion product and were able to confirm the presence of NiS. Chang [28] assumed that the rise in potential into the passive region was caused by the presence of an FeSO<sub>4</sub> film barrier. Mitsuhashi [29] theorized that the FeSO<sub>4</sub> was produced in the active region accompanied by H<sub>2</sub> evolution and that the production of the sulphate was the driving force for the passivation. In the passive region, the production of S and the H<sub>2</sub>O accompanying this production caused the FeSO<sub>4</sub> to dissolve and thus resulted in a breakdown of passivity. Kish et al. [9,26] proposed that periodic oscillations were caused by the formation and dissolution of a dense noncontinuous NiS deposit on the stainless steel surface. The reduction of H<sub>2</sub>SO<sub>4</sub> on the NiS deposit, formed at active potentials, was greater than the similar reaction on the stainless steel substrate. This generated a galvanic couple between the NiS deposit and the stainless steel, which then raised the anodic potential into the passive region. However, the NiS is not stable at passive potentials and subsequently dissolves, resulting in a loss of passivity. Upon loss of passivity, the stainless steel corrodes actively and thus the NiS deposit is formed again, continuing the cycle. While Li [10] agreed with much of the model presented by Kish, they disagreed on the structure of the NiS. Li proposed that the NiS deposit was porous and covered the passive film formed on the stainless steel while Kish argued that it was a dense noncontinuous NiS deposit. Kish proposed that it was the higher rate of reduction of H<sub>2</sub>SO<sub>4</sub> occurring on the NiS

deposit that creates a galvanic couple with the stainless steel, which raises the potential of the stainless steel into its passive region, while Li theorized that NiS catalyzes the cathodic reduction and is able to passivate the stainless steel.

Although there is a slight difference in the models presented by Kish and Li, they both postulated the formation and dissolution of the NiS corrosion product is essential for the active – passive corrosion potential oscillations exhibited by nickel containing stainless steels.

## Properties of H<sub>2</sub>SO<sub>4</sub> - H<sub>2</sub>O Systems

### *Physical and Chemical Properties*

Table 1. compares several physical properties of H<sub>2</sub>SO<sub>4</sub> and H<sub>2</sub>O, with specific regard to properties that influence the corrosivity, such as conductivity and viscosity.

Table 1: Physical properties of H<sub>2</sub>SO<sub>4</sub> and H<sub>2</sub>O [30-31]

<b>Property</b>	<b>H<sub>2</sub>SO<sub>4</sub></b>	<b>H<sub>2</sub>O</b>
Freezing Point (°C)	10.4	0
Boiling Point (°C)	290 - 317	100
Specific Conductivity (Ω <sup>-1</sup> cm <sup>-1</sup> )	1.044 X 10 <sup>-2</sup> @ 25°C	5.5 X 10 <sup>-8</sup> @ 25°C
Viscosity (cP)	25.54 @ 25°C	1 @ 25°C

The conductivity of pure H<sub>2</sub>SO<sub>4</sub> is significantly higher than pure H<sub>2</sub>O; five orders of magnitude greater at 25°C. The conductivity of H<sub>2</sub>SO<sub>4</sub> - H<sub>2</sub>O system is dependent on concentration of H<sub>2</sub>SO<sub>4</sub> and temperature [31-32]. In high

concentrations of  $\text{H}_2\text{SO}_4$  (82 – 95 wt%), the conductivity is relatively constant ( $1.25 \Omega^{-1}\text{cm}^{-1}$  at  $18^\circ\text{C}$ ) and decreases with higher concentrations of  $\text{H}_2\text{SO}_4$ , while conductivity increases with temperature for all concentrations from 0 to 100 wt%. Conductivity is important in metal corroding systems since current must flow in the electrolyte at the metal-solution interface, while electrons flow through the metal to complete the circuit. The relatively high conductivity of the concentrated  $\text{H}_2\text{SO}_4$  would indicate that metallic corrosion would not be limited by the solution resistance.

Viscosity is another physical property that can have an influence on corrosion systems. Corrosion involves transport processes, such as diffusion and convection which rely on the transport of ions and molecules in the solution, to and from the metal – solution interface. Ions and molecules have higher mobilities in solutions that are less viscous. The viscosity of pure  $\text{H}_2\text{SO}_4$  is significantly higher than pure  $\text{H}_2\text{O}$  at room temperature. However, in  $\text{H}_2\text{SO}_4$  -  $\text{H}_2\text{O}$  solutions, the viscosity decreases with a decreases in concentration of  $\text{H}_2\text{SO}_4$  and temperature [33]. The relative high viscosity of concentrated  $\text{H}_2\text{SO}_4$  -  $\text{H}_2\text{O}$  systems and its sensitivity of concentration and temperature indicate it will play a role in the corrosion of metallic materials.

$\text{H}_2\text{SO}_4$  is completely miscible in  $\text{H}_2\text{O}$  in all proportions [34]. Liler [35] summarized work done in characterizing the chemical composition of  $\text{H}_2\text{SO}_4$  -

H<sub>2</sub>O mixtures using Raman spectroscopy, the results of which are shown in Figure 2(a).

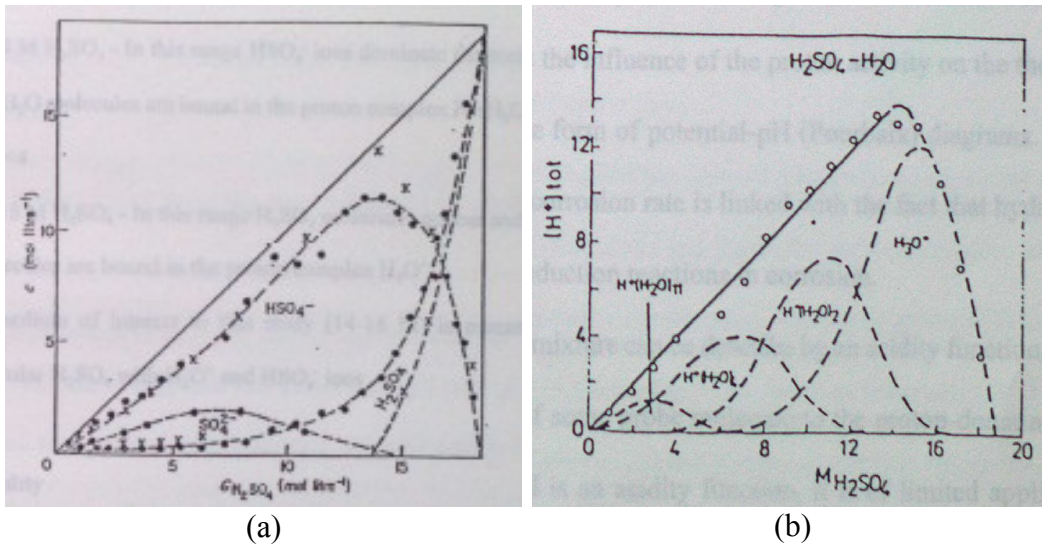
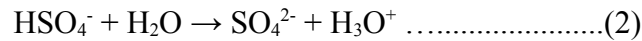
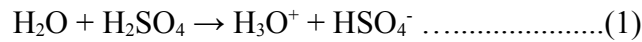


Figure 2: Chemical composition of H<sub>2</sub>SO<sub>4</sub>-H<sub>2</sub>O solutions: a) Concentration of species [35] b) Concentration and structure of hydrated protons [36]

In dilute solutions, both HSO<sub>4</sub><sup>-</sup> and SO<sub>4</sub><sup>2-</sup> ions are stable, which is consistent with the dissociation of H<sub>2</sub>SO<sub>4</sub> in H<sub>2</sub>O, shown below.



In more concentrated solutions, the solution consists of H<sub>2</sub>SO<sub>4</sub> molecules as well as H<sub>3</sub>O<sup>+</sup> + HSO<sub>4</sub><sup>-</sup> ions. Högfeldt [36] proposed that the chemical composition of H<sub>2</sub>SO<sub>4</sub> - H<sub>2</sub>O solutions can be divided into three ranges, as shown in Figure 2(b).

In dilute solutions, from 0 to 8 M (0-54 wt%), water molecules are the most

prevalent in the solution. In solutions whose concentrations range from 8 – 14 M (54-82 wt%),  $\text{HSO}_4^-$  ions dominate while at higher concentrations, 14 – 18 M (82 – 98 wt%), mostly  $\text{H}_2\text{SO}_4$  molecules are detected.

### *Electrochemical Properties*

Sridhar [37] and Banaś [38] both studied the redox potential of the  $\text{H}_2\text{SO}_4$  -  $\text{H}_2\text{O}$  systems on platinized platinum (Pt) electrodes. As shown in Figure 3, both studies found a substantial change in the redox potential at higher concentrations of  $\text{H}_2\text{SO}_4$ . The measured redox potentials in solutions having a concentration less than 8 M (54 wt%)  $\text{H}_2\text{SO}_4$  followed the predicted potential of the hydrogen evolution reaction. However, in more concentrated solutions, above 8 M (54 wt %), there was a significant change from this predicted potential. This was theorized to be the reduction of  $\text{H}_2\text{SO}_4$  molecules and  $\text{HSO}_4^-$  ions to sulphur containing compounds having a valence less than 6.

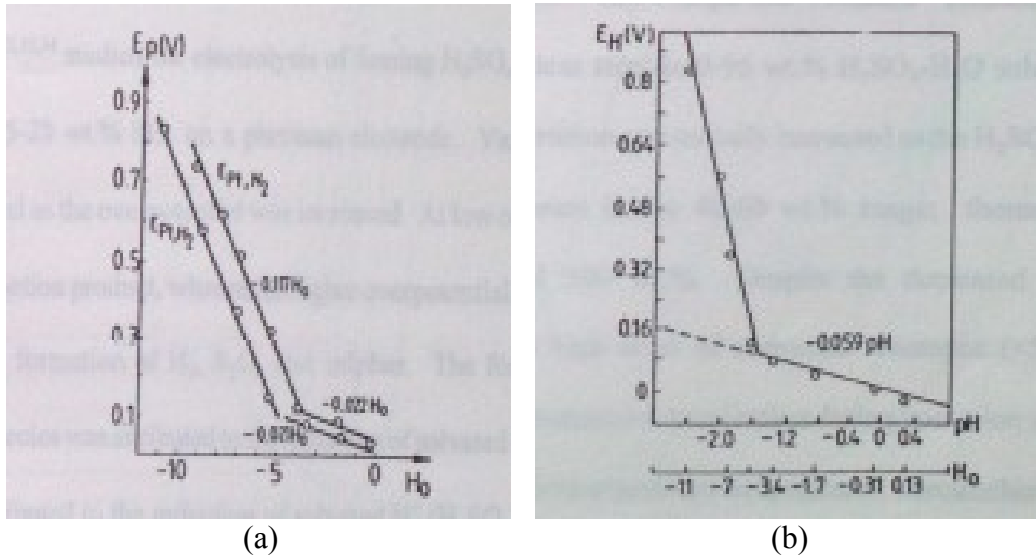


Figure 3: Redox potential of H<sub>2</sub>SO<sub>4</sub> - H<sub>2</sub>O solutions at 25 °C. a) Banaś and Stypula [38] b) Sridhar [37]

The electrolysis of H<sub>2</sub>SO<sub>4</sub> – H<sub>2</sub>O systems has been studied extensively. Beck [39] investigated the cathodic electrolysis of 85 – 100 wt% H<sub>2</sub>SO<sub>4</sub> as a function of electrode material and temperature. Beck concluded that in 80 – 95 wt % H<sub>2</sub>SO<sub>4</sub>, H<sub>3</sub>O<sup>+</sup> ions were reduced to H<sub>2</sub>, while in more concentrated solutions, 90 – 100 wt%, the H<sub>2</sub>SO<sub>4</sub> molecules were reduced to H<sub>2</sub>S, sulphur and SO<sub>2</sub>. Hoffmann [40] studied the electrolysis of 98.5 wt% H<sub>2</sub>SO<sub>4</sub> using platinum electrodes at temperatures ranging from 50 – 280 °C and found that H<sub>2</sub>S, sulphur and SO<sub>2</sub> were also formed at the cathode. Arvia et al. [41-44] investigated the electrolysis of fuming H<sub>2</sub>SO<sub>4</sub> (100 wt% H<sub>2</sub>SO<sub>4</sub> with 5 – 28 wt% of dissolved SO<sub>3</sub>) on a Pt electrode. As overpotential was increased in these systems, various

cathodic reactions were observed. At overpotentials between 0 – 0.5  $V_{Pt}$ ,  $SO_2$  was the main reaction product, while at higher overpotentials, above 0.5  $V_{Pt}$ , the reduction reaction involved the formation of  $H_2$ ,  $S_2O_3$  and sulphur.

Kish [9] conducted cathodic polarization experiments on platinum rotating disc electrodes in 93.5 wt %  $H_2SO_4$ . The cathodic polarization can be separated into 3 distinct zones indicated by 3 distinct slopes, as shown in Figure 4.

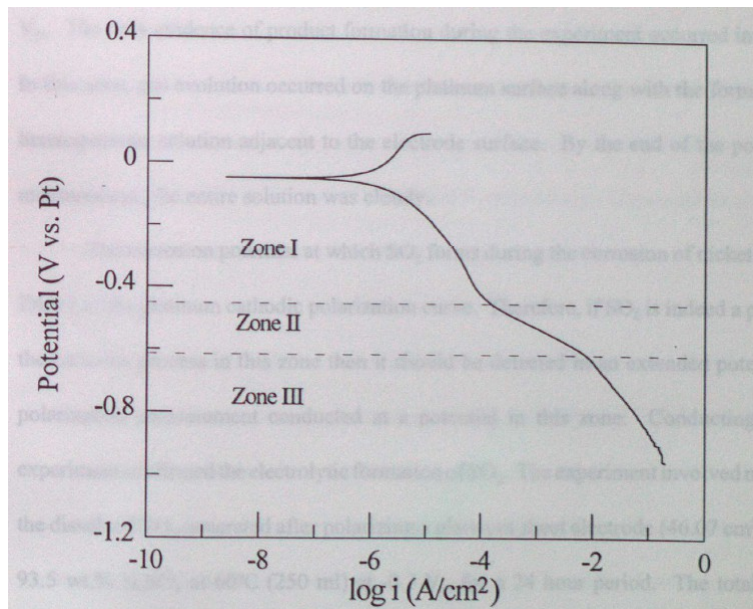


Figure 4: Potentiodynamic cathodic polarization of 93.5 wt%  $H_2SO_4$  measured on rotating platinum electrode (500 rpm) [9]

Zone I can be defined as potentials,  $E$ , above  $-0.42 V_{Pt}$ , Zone II as the section between  $-0.42$  and  $-0.60 V_{Pt}$ , and Zone III as the region below  $-0.61 V_{Pt}$ .

Kish proposed that the dominant cathodic reaction in Zone I was the electrolytic

formation of  $\text{SO}_2$ . The cathodic reaction in Zone II was the production of elemental sulphur as observations showed a yellow, water insoluble deposit on the electrode. The electrolytic production of  $\text{H}_2\text{S}$  was the dominant cathodic reaction in Zone III.

### **Anodic Protection**

Anodic protection is a field of corrosion management; its feasibility having being first established by Edeleanu in 1954 in small scale stainless steel industrial boilers for  $\text{H}_2\text{SO}_4$  solutions [45]. It has been used for storage vessels, process reactors, heat exchangers and transportation vessels that contain various corrosive solutions [5]. Anodic protection uses the phenomena of passivity to reduce corrosion rates in alloys that show passivation behaviour in a corrosive media, such as stainless steel in concentrated  $\text{H}_2\text{SO}_4$ . This is accomplished by either applying an external anodic current onto the alloy, ICAP, or by coupling the alloy to a more noble material, GCAP. Both methods aim to accomplish the same goal, which is anodically polarize the alloy such that the potential of the alloy is set within the passive region.

Anodic protection is not widely used as a corrosion control technique because its applications are limited to those metal-solution systems in which the anodic polarization of the metal will result in the formation of a protective film. In addition, even within these systems, certain design concerns must be taken into

consideration. Solution resistivity must be low enough that the overall circuit resistance is controlled by the cathode surface area and not the solution resistance [5]. Low solution resistance also ensures that the system has sufficient throwing power, ensuring that the applied current has the ability to cover complex geometries over variable distances. Incomplete passivation can result in systems that exhibit poor throwing power which can lead to catastrophic failures due to shielding effects. Also the metal being protected in such systems must have a relatively large passive potential region so that minor variations in potential along its metal surface does not result in loss of passivation. It is for these reasons that anodic protection is widely used in stainless steel – concentrated  $\text{H}_2\text{SO}_4$  systems. Concentrated  $\text{H}_2\text{SO}_4$  has shown to have high conductivity [30], while austenitic stainless steels have shown to form protective films, with large passive regions when anodically polarized [4].

#### *Impressed Current Anodic Protection (ICAP)*

ICAP has been the most extensively applied to protect equipment used to store and handle concentrated  $\text{H}_2\text{SO}_4$ , anodically protected heat exchangers being the most successful application of this technology [5]. ICAP systems are applied to tanks, piping systems and acid coolers either to diminish the extent of iron contamination in the acid and/or to reduce the corrosion rates effectively and prolong the life of the equipment. ICAP systems are a three electrode system,

where the protected stainless steel is made the anode and the current is impressed through an electrode which is made the cathode. A reference electrode is needed to monitor the potential of the stainless steel anode. ICAP systems must be properly designed, installed and maintained for the particular combinations and configuration of metal and environment [1].

ICAP systems in concentrated  $H_2SO_4$  can be used on a variety of strongly passivating alloys such as Types 304, 316, 904L, 254 SMO and Alloy 825 [1]. ICAP systems can also be used at a variety of temperatures and concentrations of  $H_2SO_4$ . Foroulis [6] conducted anodic protection feasibility studies on Type 316 stainless steel in concentrations from 3 – 92 wt %  $H_2SO_4$  and temperatures ranging from 34 °C to 121 °C. It was concluded that anodic protection was feasible for the whole range of concentrations studied to temperatures as high as 75 °C, and up to 100 °C for concentrations above 60 wt% and below 20 wt%. In addition, it was reported that for concentrations between 20- 60 wt% at 46 °C, anodic protection was able to reduce the rate of corrosion by a factor of 500.

There are many other instances in literature that have shown the protective ability of ICAP in stainless steel – concentrated  $H_2SO_4$  systems.  $H_2SO_4$  of concentrations between 96 – 98 wt% have been handled by anodically protected Type 316 heat exchangers to temperatures up to 110 °C. Corrosion rates in these systems have been reduced from 5 mm/y to less than 0.025 mm/y. [5].

Munro et al. [46] reported that the corrosion rate of Type 316 exposed to 93 wt% and 98 wt% H<sub>2</sub>SO<sub>4</sub> was greatly reduced by anodic protection at 70 °C and 100 °C. At 70 °C, the corrosion rate of Type 316 was reduced from 0.74 mm/y to less than 0.05 mm/y when exposed to 93 wt% H<sub>2</sub>SO<sub>4</sub>, and reduced from 12.6 mm/y to 0.64 mm/y at 100 °C. While at 100 °C in solutions of 98 wt% H<sub>2</sub>SO<sub>4</sub> the corrosion rate was reduced from 1.04 mm/y to less than 0.05 mm/y when anodic protection was applied. In addition, in solutions of 99 wt% H<sub>2</sub>SO<sub>4</sub> at 160 °C the corrosion rate of Type 316L was reduced from 110 mm/y to 0.2 mm/y via the application of anodic protection [1].

ICAP systems accomplish the passivation of stainless steel by externally applying a current onto the stainless steel via a cathode. In order to passivate the stainless steels, the  $i_{crit}$  of the stainless steel must be exceeded by the impressed current. Depending on the surface area of the stainless steel being protected, this can require large amount of current. This must be done quickly as well, since the  $i_{crit}$  is proportional to the highest corrosion rate and anodic dissolution is significantly accelerated in the region around the  $i_{crit}$ . Once the critical current density has been passed, only a small current density is require to maintain passivity in the system as shown in Table 2. In addition, too much current can cause the stainless steel to be polarized into the transpassive region and can result in increased corrosion.

Table 2: Current density require to passivate and maintain passivity of a variety of alloys in different concentrations of sulphuric acid [5]

<b>H<sub>2</sub>SO<sub>4</sub> Concentration</b>	<b>Alloy</b>	<b>Current Density</b>	
		<b>To passivate (mA/cm<sup>2</sup>)</b>	<b>To maintain (mA/cm<sup>2</sup>)</b>
67 wt%	304	5.1	0.0034
67 wt%	316	0.51	0.0010
93 wt%	Mild Steel	0.28	0.0230

The cathode used in ICAP systems is connected to the negative pole of the power source and completes the electrical circuit. A number of factors must be taken into the consideration when considering a cathode material such as size, cost and long term stability [4]. Cathode size is chosen according to the geometry of the vessel being protected and are designed to have the largest surface area possible in order to reduce overall resistance in the system. As such, cathode materials must have a high conductivity that does not contribute to the overall circuit resistance. Since large surface areas are needed for the cathodes, there is an incentive to use less costly materials. A number of materials have been used for cathodes in ICAP systems for H<sub>2</sub>SO<sub>4</sub> applications and some are listed in Table 3.

Table 3: Cathode materials used in ICAP systems for sulphuric acid applications [5,7-8]

<b>Cathode Material</b>	<b>H<sub>2</sub>SO<sub>4</sub> Concentration</b>
Platinum-clad brass	Various
Chromium nickel steel	78 – 105 wt%
Silicon cast iron	89 – 105 wt%
Hastealloy C	Various
N06200	93 – 94 wt%
N10665	98 – 99 wt%

Pt-clad brass electrodes are electrochemically stable and are of a permanent type. However, industry has moved away from such electrodes due to their high costs. Hastealloy C, a chromium nickel alloy, has been used in a few H<sub>2</sub>SO<sub>4</sub> applications. This alloy, however, has a limited life in H<sub>2</sub>SO<sub>4</sub> heat exchangers, having to be replaced ever three to four years [4]. Rodda et al [7-8] showed that corrosion was accelerated in N06200 and N10665 alloys, commonly used as cathodes in anodically protected stainless steel heat exchangers, under cathodic polarization. It occurred over a limited range of current densities larger than those typically required to establish and maintain protection of an anodic structure during normal operations. In addition, Rodda et al. found sulphur deposits on cathodes during cathodic polarization on a number of alloys tested. Elemental sulphur is insoluble in concentrated H<sub>2</sub>SO<sub>4</sub> and is also electrically insulating. As such it is not desirable to form sulphur under cathodic polarization for alloys used as cathodes in ICAP systems.

Reference electrodes used for anodic protection should be physically rugged, relatively stable in the corrosive liquid. They must also have a potential that is stable with respect to time, temperature and solution composition [4]. For use in concentrated  $H_2SO_4$ , the most commonly used reference electrodes are  $HgCl_2$ ,  $Ag/AgCl$  and  $Hg/HgSO_4$  and Pt [4,5]. These reference electrodes are able to accurately measure the potential of the anode and compare it to the set passive potential. Reference electrodes work as a part of a potential control system in conjunction with direct current power supply to ensure that the correct amount of current is being applied to the cathode to protect the anode. Since there is often a significant difference between the amount of current needed to passivate the system and the amount of current needed to maintain passivity, a power supply is needed that can handle both high output, as well as much lower outputs of power. In recent years, potential control systems have been changed from simple on-off systems to continuous proportional-type controls [4]. The combination of the sophisticated proportional-type controls and the need for specialized power supplies make these potential control systems relatively expensive and complex [4].

#### *Galvanic Couple Anodic Protection (GCAP)*

GCAP systems provide some advantages over ICAP systems. GCAP systems are a self – passivating system, no external current is needed to passivate

the anode. Secondly, a GCAP is a less complex system than an ICAP system, since a GCAP system are a two electrode system as compared to an ICAP system, which is a three electrode system. In a GCAP system, a reference electrode is used only to monitor the system, since there is no need for potential control from applied current, which likely reduces complexity and cost. Lastly, if a cathode material is used whose open circuit potential is less than the transpassive potential of the anode, transpassive corrosion is not possible in a GCAP system. GCAP systems are not widely utilized and little research has been done on the subject.

GCAP systems exploit galvanic corrosion in order to protect the anode in the systems. A galvanic cell is formed when two dissimilar metals are connected electrically while both are immersed in an electrolyte. When the two metals are connected, the more active metal, having a more negative corrosion potential, has an excess of electrons which are lost to the more noble alloy, having a more positive corrosion potential. The more active metal becomes the anode in the galvanic cell and the more noble metal, the cathode. While galvanic coupling is most often detrimental in corrosion engineering as it usually means an increase in corrosion rates of the more active metal, there are instances where galvanic coupling may be beneficial in reducing corrosion rates in metallic materials that show anodic passivation behaviour.

In general, galvanically coupling two dissimilar metals, neither of which

show anodic passivation, will result in the more active metal corroding faster. These changes can be explained by anodic and cathodic polarization within the galvanic couple. When uncoupled, the active metal establishes a corrosion potential,  $E_{\text{corr,a}}$ , and noble metal establishes a its own corrosion potential,  $E_{\text{corr,n}}$ . When coupled together, the electrons flow from the active metal to the noble metal, thus polarizing both surfaces. The surface of both metals polarize to the same potential,  $E_{\text{couple}}$ , where the total reductive current is equal to the total oxidation current as required by “mixed potential” theory, in order to avoid charge accumulation in the electrodes. Coupling the two metals together results in the potential of the active metal being shifted to a more noble potential and the corrosion rate of the active metal is increased.

Titanium (Ti), shows anodic passivation behaviour in dilute acid solutions and when galvanically coupled to Pt or Ni, the corrosion rate of the Ti will be reduced. When uncoupled, the Ti establishes a corrosion potential,  $E_{\text{corr}}$ , which falls in its active state, and thus it corrodes rapidly, while Pt establishes an open circuit potential at a more noble potential. When coupled, the reduction current is greater than the oxidation current needed for passivation and, thus the Ti is anodically polarized in to the passive region. Since the reduction current is also greater than the  $I_{\text{crit}}$  needed for passivation, during the anodic polarization, a protective oxide film is formed on the Ti. The couple potential,  $E_{\text{couple}}$ , is

established in the passive region of Ti, where the corrosion rate of the Ti is significantly less than the corrosion rate when uncoupled [47]. A schematic of this behaviour is shown in Figure 5.

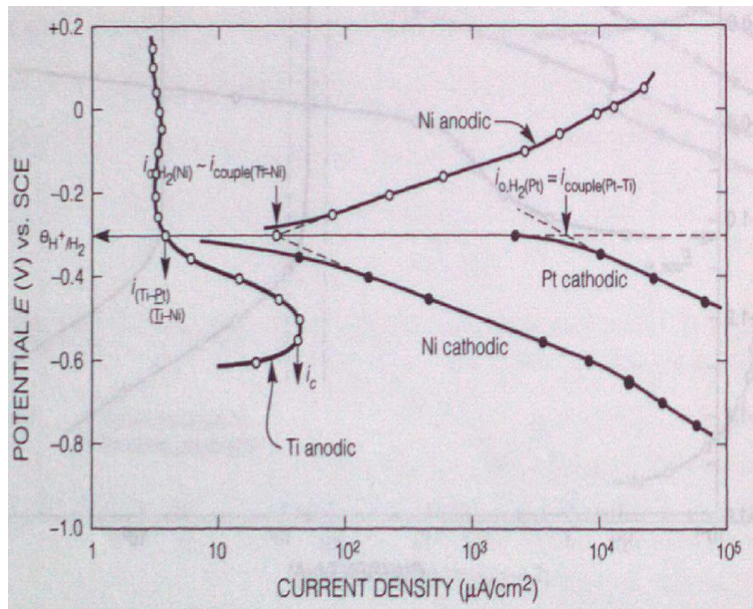


Figure 5: Schematic of Ti coupled to Pt and Ni [47]

Bianchi et al. [48] studied the efficiency of the anodic protection of Type 304, by coupling it to Pt at a variety of temperatures and concentrations of H<sub>2</sub>SO<sub>4</sub>. They concluded that galvanically coupling Pt to the stainless steel is able to passivate the stainless steel because the Pt displayed a lower overvoltage of both hydrogen-ion discharge and for the cathodic reduction of oxygen. The relative surface areas of the cathode and anode contributes significantly in a galvanic

couple, and, thus particular attention was paid to minimum cathode/anode surface ratio,  $R$ , needed to passivate the stainless steel. The corrosion rate of the stainless steel when coupled to Pt was recorded for a range of surface area ratios,  $R$ , from 0.01 to 100 in 40 wt%  $H_2SO_4$  at 25 °C. For  $R$  greater than 1.0, the cathodic current of the reduction of oxygen was greater than the  $I_{crit}$  needed to passivate the stainless steel and the corrosion rate was drastically reduced to less than 1  $mg/cm^2$ , when compared to 4  $mg/cm^2$  at  $R=0.1$ . Shown in Figure 6. are the minimum cathode/anode ratios needed to passivate the stainless steel at a variety of temperatures and acid concentrations. At higher temperatures, larger cathode/anode ratios are needed in order to overcome the  $I_{crit}$  needed to passivate the stainless steel. The largest cathode/anode ratios are needed for acid solutions between 63.8 wt% and 74 wt%  $H_2SO_4$ .

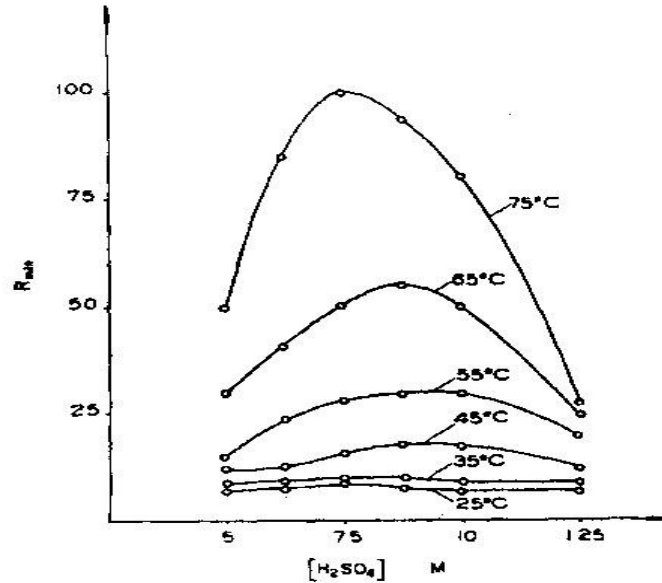


Figure 6: Surface area ratios needed to passivate S30400 with platinum at a variety of temperatures and concentrations of sulphuric acid [48]

Nakahara et al. [49] reported that noble materials, such as Pt and Au, were able to improve the corrosion performance of Type 316 stainless steel when galvanically coupled in an industrial application. Type 316 was shown to show potential oscillations when immersed in concentrated H<sub>2</sub>SO<sub>4</sub>, 95 – 100 wt%, and have an overall corrosion rate of 0.005 mm/y when uncoupled. Type 316 coupled to Pt at an anode/cathode surface area ratio of 150:1 in 100 wt% H<sub>2</sub>SO<sub>4</sub> in a laboratory test showed that the potential of the Type 316 was stabilized, showing no potential oscillations, and the potential of the stainless steel was ennobled from 0.3V<sub>Pt</sub> to 0.45V<sub>Pt</sub>. The potential stability was maintained for 120 h after coupling.

Due to the high cost of Pt, Au plated Type 316 electrodes were used in a working plant. A anode/cathode surface ratio of 150:1 was used, resulting in a cessation of process parameters fluctuations and normalized productivity. After two months of operation, there was no signs of thinning of the Au plated electrode or any signs of delamination of the Au layer.

As large cathodes needed for anodic protection systems, there is an incentive to produce low costs cathodes. So far, it has been shown that noble metals, such as Pt and Au, have been able to protect stainless steels of different grades when galvanically coupled. However, these materials are expensive, yet viable, less expensive cathode materials are sought. Zhong et al. [50] were able to develop a galvanic anodic protection (GAP) system using polyaniline (PANI) film electrode that was able to protect 1Cr13 ( 0 – 15% C, 13% Cr) stainless steel in 38. wt% H<sub>2</sub>SO<sub>4</sub> at 25 °C. When coupled to 1Cr13 stainless steel at a ratio of 2:1, the PANI electrode was able to passivate the stainless steel for 120 h. After 120 h, the mixed potential fell below 0 V<sub>Pt</sub> and the stainless steel started to corrode actively. When a ratio of 1:1 was used, the PANI electrode was able to passivate the stainless steel for over 200 h.

Kish [9] conducted an experiment in which Type 430 was galvanically coupled to a NiS(Ni) electrode, NiS grown in situ on a Ni substrate, in 93.5 wt% H<sub>2</sub>SO<sub>4</sub> at 60 °C. Samples of equal surface areas were coupled and uncoupled in 15

minute intervals and the potential on the stainless steel was recorded. The results of this experiment are shown in Figure 7.

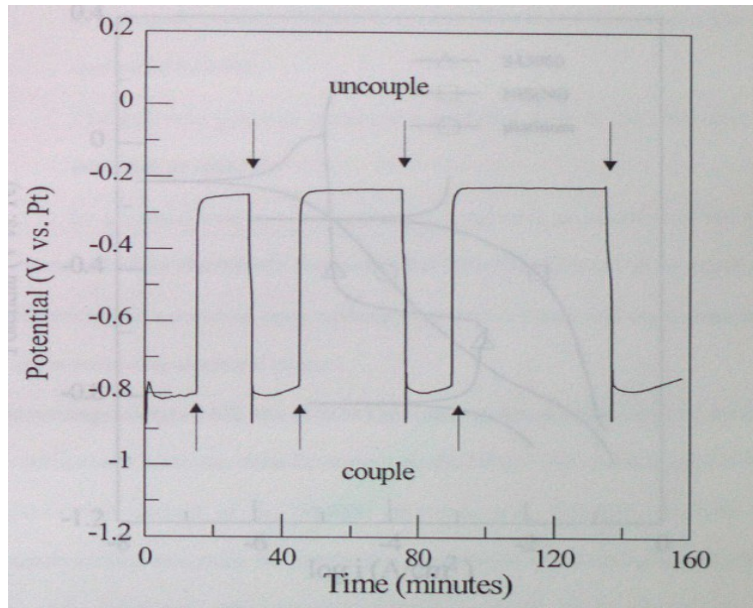


Figure 7: Potential readings during Type 430 - NiS(Ni) couple experiment [9]

The coupling of the NiS(Ni) to the Type 430 was able to polarize the stainless steel into its passive region as shown by the ennobling of the potential on the stainless steel from about  $-0.8 V_{Pt}$  to about  $-0.25 V_{Pt}$  where it remained stable for the duration of the couple. When uncoupled, the stainless steel returned to its uncoupled corrosion potential and corroded actively. Weight loss experiments were conducted by galvanically coupling the NiS(Ni) electrode to a stainless steel electrode for 4 h at the same conditions, while also exposing an

uncoupled stainless steel electrode to the same conditions. The uncoupled samples showed a weight loss of  $3.69 \text{ mg/cm}^2$  while the galvanically coupled sample showed a weight loss of only  $0.03 \text{ mg/cm}^2$ , a reduction of two orders of magnitude.

However, no long term tests were done to find how long this NiS(Ni) electrode was able to passivate the stainless steel. Long term exposure of the NiS(Ni) electrode in 93.5 wt%  $\text{H}_2\text{SO}_4$  at  $60^\circ\text{C}$  showed a single potential oscillation as shown in Figure 8.

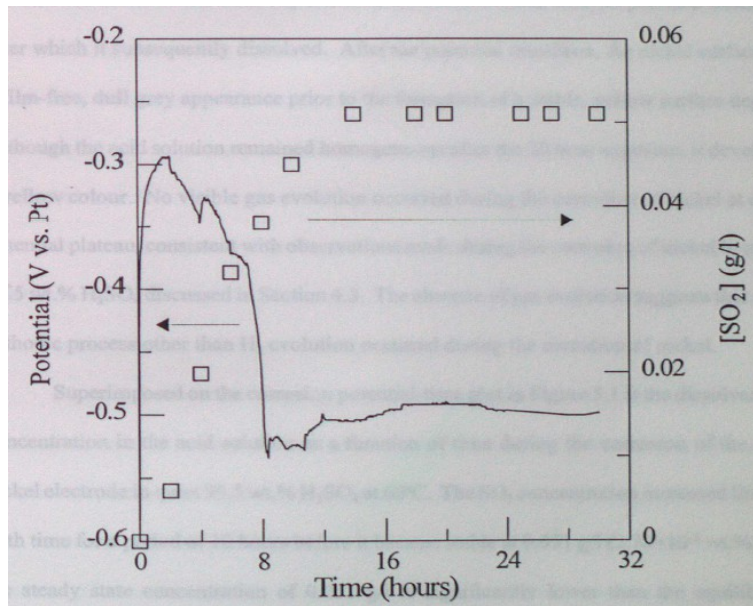


Figure 8: Corrosion potential of nickel electrode as a function of time in 93.5 wt%  $\text{H}_2\text{SO}_4$  at  $60^\circ\text{C}$  [9]

During the first hour of exposure, the potential on the Ni electrode quickly

reached a maximum of about  $-0.3 V_{Pt}$ . A solid black NiS deposit was formed on the surface of the electrode after immersion and covered most of the sample. After the first hour of exposure, the sample showed a slow decay lasting about 8 h before finally stabilizing at a potential of about  $-0.5 V_{Pt}$ . During this decay, the NiS film dissolves and after 8 h the nickel surface had a film free, dull grey appearance indicating that NiS film has likely dissolved. This experiment showed that the NiS film is not stable for long term exposures. This is because the NiS is relatively thin and once it is removed the Ni is exposed to the  $H_2SO_4$  and this is reflected in the drop in the potential.

### **Galvanic Effect in Metal Sulphides**

The galvanic effect of transition metal sulphides on one another and metals has been examined in hydrometallurgy. It is said to be one of the most important electrochemical factors that governs the dissolution rate of transition metal sulphide minerals [56]. In nature, most metal sulphide minerals have semiconductor properties and possess low electric resistivities [52]. Table 4 shows the electric resistivity of the most commonly found metal sulphides, as well as NiS.

Table 4: Electric Resistivities of a number of metal sulphides

<b>Mineral</b>	<b>Formula</b>	<b>Electric Resistivity (ohm cm)</b>
Pyrite[53]	FeS <sub>2</sub>	0.005 - 5
Chalcopyrite[53]	CuFeS <sub>2</sub>	0.01 – 0.07
Galena[53]	PbS	0.003 – 0.03
Millerite [54]	NiS	0.00005

Galvanic interactions can occur between electrically conducting minerals are in contact with one another and are present in an electrolyte. The galvanic interactions arise due to the different electrochemical reactivities of the sulphides, which are indicated by their rest potential ( $E_{\text{corr}}$ ) and change the rates of the anodic and cathodic half-reactions that occur at the surface of each mineral [55-56]. The mineral with the higher rest potential ( $E_{\text{corr}}$ ) acts as the cathode, which is galvanically protected, while the mineral with the lower rest potential ( $E_{\text{corr}}$ ) acts as an anode and its dissolution is favored through electronic interactions [58]. Metha and Murr [60] studied the rest potentials of some sulphide minerals with respect to the the standard hydrogen electrode and their results are presented in the Table 5.

Table 5: Rest potentials of some sulphide minerals [60]

<b>Mineral</b>	<b>Chemical formula</b>	<b>Rest potential (<math>V_{SHE}</math>)</b>
Pyrite	FeS <sub>2</sub>	0.63
Chalcopyrite	CuFe <sub>2</sub>	0.52
Chalcocite	Cu <sub>2</sub> S	0.44
Covellite	CuS	0.42
Galena	PbS	0.28
Sphalerite	ZnS	-0.24

It has been reported that galena (PbS), sphalerite (ZnS) and covellite (CuS) oxidized 8 – 20 times faster when pyrite (FeS<sub>2</sub>) is present [57]. Rao and Finch [55] conducted galvanic interaction studies on a number of different sulphide minerals. They found that the potentials of FeS<sub>2</sub> – PbS and FeS<sub>2</sub> – ZnS couples were lower than the rest potential of FeS<sub>2</sub>, and this is explained by the galvanic interactions between the sulphide minerals. The FeS<sub>2</sub> acting as the cathode drew electrons from the PbS or ZnS and thus the potentials of the couples was less than the rest potential of the FeS<sub>2</sub>. Koleini et al. [59] studied the leaching behaviour of CuFe<sub>2</sub> concentrates in the presence of FeS<sub>2</sub> in an acidic sulphate solution. They reported that the addition of FeS<sub>2</sub> had a major catalytic effect on the CuFe<sub>2</sub> due to the formation of a galvanic cell between the minerals which was caused by the difference in their rest potential. A mass ratio of 2:1 for FeS<sub>2</sub> to CuFe<sub>2</sub> minerals was found to be the optimum ratio to obtain maximum Cu recovery. Holmes and Crundwell [56] investigated the galvanic interaction between Cu and FeS<sub>2</sub> in an

acidified sulphate solutions. In such a system, the FeS<sub>2</sub> forms the cathode and the Cu the anode. They reported that the anodic dissolution of the Cu was an electrochemically controlled reaction while, the reduction of Fe<sup>3+</sup> ions on the FeS<sub>2</sub> cathode was observed to be controlled by electrochemical and mass transfer processes.

### **Summary**

A critical review of the literature was conducted and the following assessments are made. The passive film formed on the stainless steels in concentrated H<sub>2</sub>SO<sub>4</sub> solutions is a thin, three-dimensional chromium-rich oxide-hydroxide. Ni containing austenitic stainless steels have been found to exhibit spontaneous periodic active – passive potential oscillations when exposed to concentrated H<sub>2</sub>SO<sub>4</sub>. The cause of the oscillations observed is the periodic production and dissolution of an intermediate corrosion product, NiS, formed during active corrosion. The physical and electrochemical properties of H<sub>2</sub>SO<sub>4</sub> – H<sub>2</sub>O solutions were outlined. ICAP systems have been extensively applied to protect equipment used to store and handle H<sub>2</sub>SO<sub>4</sub>, including stainless steel heat exchangers. While effective at controlling corrosion in H<sub>2</sub>SO<sub>4</sub> manufacturing, ICAP systems have a number of issues. They require a constant source of current to ensure reliable corrosion; they are relatively complex systems and expensive to install; improper potential control can lead to loss of corrosion protection; and

they have some issues with cathode fouling and erosion have been reported. GCAP systems have not been widely utilized, but offer some solutions to these issues. GCAP systems have been developed to effectively protect stainless steel in concentrated  $H_2SO_4$  solutions using Pt and Au as the cathode materials. More inexpensive cathode materials such as PANI have been used, but are much less effective. The ability of metal sulphides such as NiS, to form galvanic couples has been shown, thus suggesting the such metal sulphides could be used in GCAP systems.

## **CHAPTER 3**

### **Experimental Details**

#### **Materials and Solution**

##### *Metals*

A ferritic stainless steel, Type 430, sheet, having a thickness of 3 mm, was used to fabricate electrodes for experimentation. The stainless steel was used in the as-received, solution annealed condition, from the manufacturer (ThyssenKrupp Materials). Glow discharge optical emission spectroscopy (GDOES) analysis of 2 samples of the stainless steel yielded an average composition, shown in Table 6.

*Table 6: Average composition of samples vs. standard composition of Type 430*

<b>%(a)</b>	<b>C</b>	<b>Mn</b>	<b>Si</b>	<b>Cr</b>	<b>Ni</b>	<b>P</b>	<b>S</b>
<b>Standard</b>	0.12	1	1	16.0 – 18.0	0.05	0.04	0.03
<b>Sample</b>	0.12	0.2	0.19	16.9	0.04	0.03	0.03

99.9 wt% commercially pure Ni (Hypertron Inc.) 1.6 mm sheet and 99.9 wt% 0.5 mm foil (Goodfellow Metals) were used in the as-received, cold rolled and annealed condition.

### *Nickel Sulphide*

A NiS sample was created by the Brockhouse Institute for Materials Research, McMaster University. The electrode was created by reacting 5.9 g of reagent grade nickel powder and 3.2 g of reagent grade sulfur powder in a vacuum sealed quartz tube. The sample was then heated, readily reacting at 600 °C. At 900 °C, the material in the tube coalesced together to form a monolithic sample and was then allowed to cool down to room temperature.

A small part of the NiS sample was characterized using two-dimensional X-ray diffraction (XRD<sup>2</sup>) using a 2D CCD detector by the McMaster Analytical X-ray Diffraction Facility, McMaster University. A Smart 6000 system by Bruker AXS Inc. with a Cu rotating anode source ( $\lambda = 1.54184 \text{ \AA}$ ) was used. The X-ray beam diameter was 500  $\mu\text{m}$ , the detector distance was 16.715 cm and was calibrated with alumina, Al<sub>2</sub>O<sub>3</sub>. Data was collected from 4 fixed 2 $\theta$  swing angles.

At each swing angle, the sample was exposed for 5 min and rotated  $60^\circ$  around  $\phi$ . The results are shown in Figure 9 (a). The data was processed using GADDS (General Area Detector Diffraction System) software by Bruker AXS Inc. A  $\chi$  integration was then conducted using GADDS over the  $2\theta$  range of  $8^\circ$  to  $100^\circ$  to obtain an intensity vs  $2\theta$  graph. Topas software by Bruker AXS Inc. was used to analyze the obtained diffraction pattern, shown in Figure 9 (b). Single crystal analysis was conducted to find the crystal structure of the electrode, specifically space group and lattice parameters. These were found to be in agreement with the ICSD (Inorganic Crystal Structure Database) database for nickel sulphide (NiS) [51]. This information was used in Topas along with 2 preferred orientations to match the pattern obtained during the X-ray diffraction.

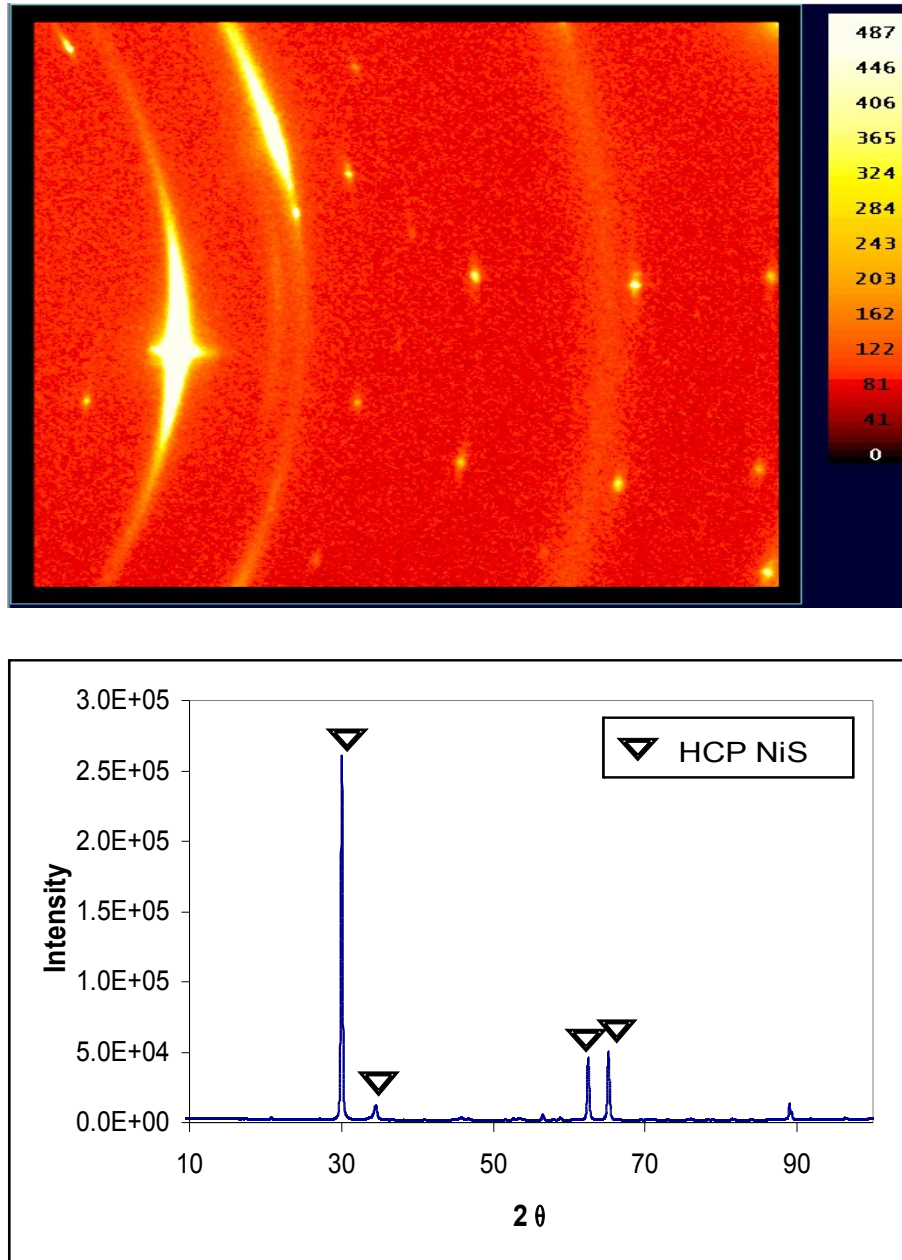


Figure 9: a) XRD<sup>2</sup> analysis of NiS sample. b) Single crystal analysis of NiS Sample

### *Solution*

93.5 wt%  $\text{H}_2\text{SO}_4$  was used in all experiments and was created by diluting reagent grade (Caledon),  $\text{H}_2\text{SO}_4$ , using deionized water. The concentration of the created solution was then analyzed using an ultrasonic sound velocity measurements with a Nusonics Inc. Model 6080 concentration analyzer and verified to be the required concentration using a calibration chart developed in the Walter Smeltzer Corrosion Laboratory, McMaster University. No effort was made to aerate or deaerate the solution during experiments and a virgin acid solution was used for each experiment. At the elevated temperatures, a heating mantle was used and temperature was controlled using a Cole-Parmer Digi-Sense Temperature Controller and verified by a thermometer.

### **Electrode Preparation**

#### *Mounted Electrodes*

Circular electrodes were cut from a sheet of Type 430 of thickness 3 mm and a diameter of 15.9 mm. Similar diameter circular electrodes were cut from a pure Ni sheet of a thickness of 1.6 mm. The surfaces of the samples were prepared using 400-grit emery paper to produce a consistent surface finish. The samples were then rinsed in deionized  $\text{H}_2\text{O}$  and methanol,  $\text{CH}_3\text{OH}$ . They were loaded into a Princeton Research K105 Flat Specimen holder<sup>®</sup> with a Kalrez<sup>®</sup> washer, shown in Figure 10, which exposes a flat surface of the stainless steel, 1

cm<sup>2</sup> in area,. These electrodes were used for polarization tests and some galvanic couple tests.



*Figure 10: Princeton Research K105 Flat Specimen holder® with a Kalrez® washer*

### ***Suspended Electrodes***

4 Type 430 samples of varying surface areas was machined from a sheet of Type 430 of thickness 3 mm having surface areas of 7.5 cm<sup>2</sup>, 10 cm<sup>2</sup>, 75 cm<sup>2</sup> and 100 cm<sup>2</sup> respectively and their surfaces were prepared by using 400-grit emery paper as well. The samples were then rinsed in deionized H<sub>2</sub>O and CH<sub>3</sub>OH. The 7.5 cm<sup>2</sup> and 75 cm<sup>2</sup> samples were used to conduct the surface area galvanic couple tests with the NiS electrode, while the 10 cm<sup>2</sup> and 100 cm<sup>2</sup> samples were used for the galvanic couple tests with the NiS(Ni) electrodes. Three Ni electrodes of varying surface areas was machined from a foil of 99% Ni having a thickness of 0.5 mm having surface areas of 47.3 cm<sup>2</sup>, 24 cm<sup>2</sup> and 5 cm<sup>2</sup> respectively and their surfaces were prepared by using 400-grit emery paper . The samples were then

rinsed in deionized H<sub>2</sub>O and CH<sub>3</sub>OH and these electrodes were used for the galvanic couple shielding tests. Examples of these types of electrodes are shown in Figures 11 and 12.

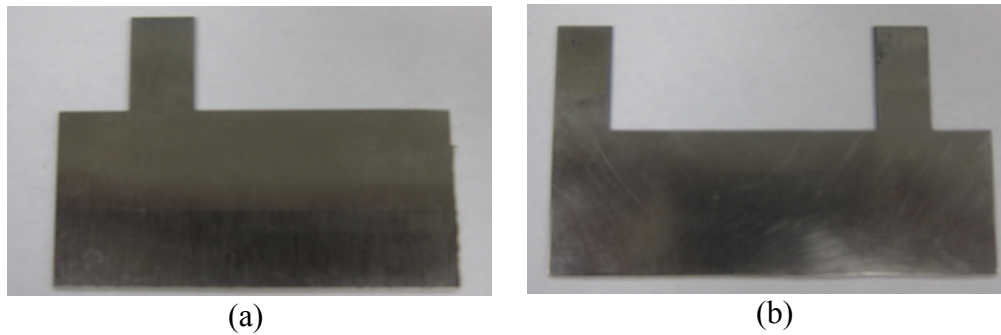


*Figure 11: Examples of suspended Type 430 electrodes; a) 75 cm<sup>2</sup>, b) 100 cm<sup>2</sup>*

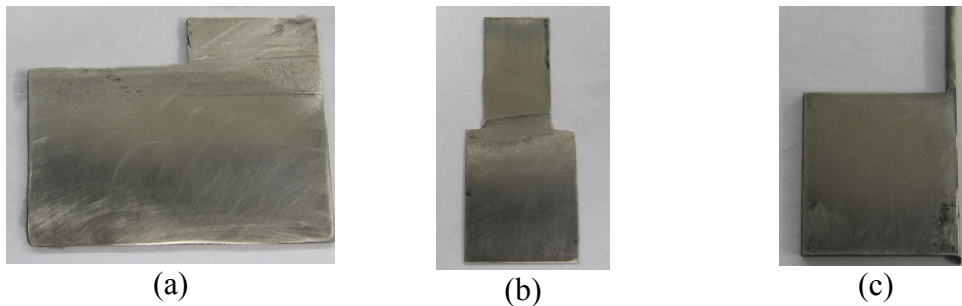


*Figure 12: Examples of suspended NiS(Ni) electrodes; a) 47.3 cm<sup>2</sup>, b) 24 cm<sup>2</sup> c) 5cm<sup>2</sup>*

An array of stainless steel coupons were machined from 3 mm thick plate of Type 430 and configured so that there were 20 coupons arranged in the 3 rows, 7 coupons in the first and last rows and 6 in the middle row. The coupons were 2 cm in the width and spaced 1 cm apart from each other. The stainless steel

surfaces were prepared by using 400-grit emery paper and then cleaned in deionized H<sub>2</sub>O and CH<sub>3</sub>OH. This array was used in the shielding experiments conducted with NiS(Ni) electrodes.

### *NiS Electrode*

The NiS sample was bonded to a Cu wire with epoxy and encapsulated in high density polyethylene, HPDE. The sample was then ground down to expose a flat surface, 0.76 cm<sup>2</sup> in area, to create the electrode, which is shown in Figure 13. The electric conductivity of the bonded joint was tested with an ohmmeter and showed negligible resistance. The surface was prepared by using 400-grit emery paper and then rinsed in deionized H<sub>2</sub>O and CH<sub>3</sub>OH.



*Figure 13: Exposed Surface of NiS electrode*

## **Electrochemical Tests**

### *Open Circuit Potential Measurements*

Electrochemical measurements to determine the open circuit potential of

the NiS, NiS(Ni) and stainless steel electrodes were made using a two electrode setup; a Koslow mercurous sulphate (Hg/Hg<sub>2</sub>SO<sub>4</sub>) electrode (MSE) with a potential of 0.513 V<sub>SHE</sub> was used as the reference electrode. In order to record the potentials observed either a Gamry Instruments PC4 Potentiostat/Galvanostat and Framework software V1.0 or a voltmeter was used. This setup was used to record potentials during the galvanic couple experiments and shielding experiments.

### *Polarization Measurements*

Electrochemical measurements to determine the polarization behaviour of the NiS electrode, NiS(Ni) and stainless steel mounted electrodes. The electrodes were placed in a 1 L electrochemical cell filled with virgin acid. A typical three electrode setup was used, a Koslow mercurous sulphate (Hg/Hg<sub>2</sub>SO<sub>4</sub>) electrode (MSE) with a potential of 0.513 V<sub>SHE</sub> was used as a reference electrode and a coil of Pt wire was used at the counter electrode.

Potentiodynamic scans were conducted on the Type 430 starting at the corrosion potential and polarized in a positive direction at a rate of 0.1666 mV/s at both room temperature and 60 °C. The stainless steel samples were exposed to the solution for 1 h before being anodically polarized. The NiS electrode was exposed to the acid for 1 h as well before being cathodically polarized. The scans started the open circuit potential of the NiS electrode and polarized in a negative

direction at a rate of 0.1666 mV/s at both room temperature and 60 °C. While the NiS(Ni) electrodes were exposed for 1 h at 60 °C and for 3 h at room temperature, in order for the NiS film to be formed, before the potentiodynamic scans were conducted. Potentiodynamic scans were done on the NiS(Ni) electrodes starting at the open circuit potential of the electrodes and polarized in a negative direction at a rate of 0.1666 mV/s at both room temperature and 60 °C.

## **Galvanic Couple Tests**

### ***Surface Area Relationship: NiS – Type 430***

In order to test the minimum surface area ratio needed to passivate Type 430 using the NiS electrode a galvanic couple experiment was conducted at room temperature. The NiS electrode was placed in a HDPE tank, 26 cm by 27 cm by 14 cm, filled with 4 liters of virgin acid, and exposed for 1 h at room temperature. A Type 430 electrodes, having a surface area of 7.5 cm<sup>2</sup>, in order to get a 10:1 anode/cathode surface area ratio, were placed 20 cm away from the NiS electrode in the tank for 1 h before the galvanic coupling experiments were conducted. A Gamry Instruments PC4 Potentiostat/Galvanostat and Framework software V1.0 and a voltmeter was used during the electrochemical measurements to measure the open circuit potential of the NiS electrode and Type 430 electrode, respectively. The potentials on both electrodes was recorded for 5 min, then

electrically connected with a Cu wire for 10 min and then uncoupled for 5 min. This process was repeated for the electrode of Type 430 having a surface area of 75 cm<sup>2</sup> using virgin acid, in order to get a 100:1 anode/cathode surface area ratio.

#### *Surface Area Relationship: NiS(Ni) – Type 430*

Another galvanic couple experiment was conducted at room temperature to determine the surface area ratio needed to passivate Type 430 using a NiS(Ni) electrode. A mounted NiS(Ni) electrode was placed in a HDPE tank filled with virgin acid, and exposed for 4 h at room temperature. A Type 430 electrode, having a surface area of 10 cm<sup>2</sup>, in order to get a 10:1 anode/cathode surface area ratio, was placed 20 cm away from the NiS electrode in the tank for 1 h before the galvanic coupling experiments were conducted. A Gamry Instruments PC4 Potentiostat/Galvanostat and Framework software V1.0 was used during the electrochemical measurements to measure the open circuit potential of the NiS(Ni) and Type 430 electrodes. After 1 h, the potentials on both electrodes was recorded for 5 min, then electrically connected with a Cu wire for 10 min and then uncoupled for 5 min. This process was repeated for the electrode of Type 430 having a surface area of 100 cm<sup>2</sup> using virgin acid, in order to get a 100:1 anode/cathode surface area ratio. An example of this experiment is shown in Figure 14.



*Figure 14: Galvanic couple surface area experiment*

### ***Shielding Experiments***

In order to observe whether there would be shielding effects in the GCAP system, an experiment was conducted at room temperature using a Type 430 – NiS(Ni) couple. The stainless steel array of coupons were suspended in a HDPE tank of virgin acid so that 5 cm of the coupons were submerged in the acid exposing a total surface area of  $472 \text{ cm}^2$ . The stainless steel array were arranged as shown in Figure 15. A NiS(Ni) electrode having a surface area of  $47.3 \text{ cm}^2$ , in order to get a 10:1 anode/cathode surface area ratio, was placed in a HDPE tank filled with 4L of virgin acid, and exposed for 4 h at room temperature. The

NiS(Ni) electrode was placed 10 cm from the first row of stainless steel coupons, the second row placed 5 cm from the first and the third row 5 cm away from the second row.

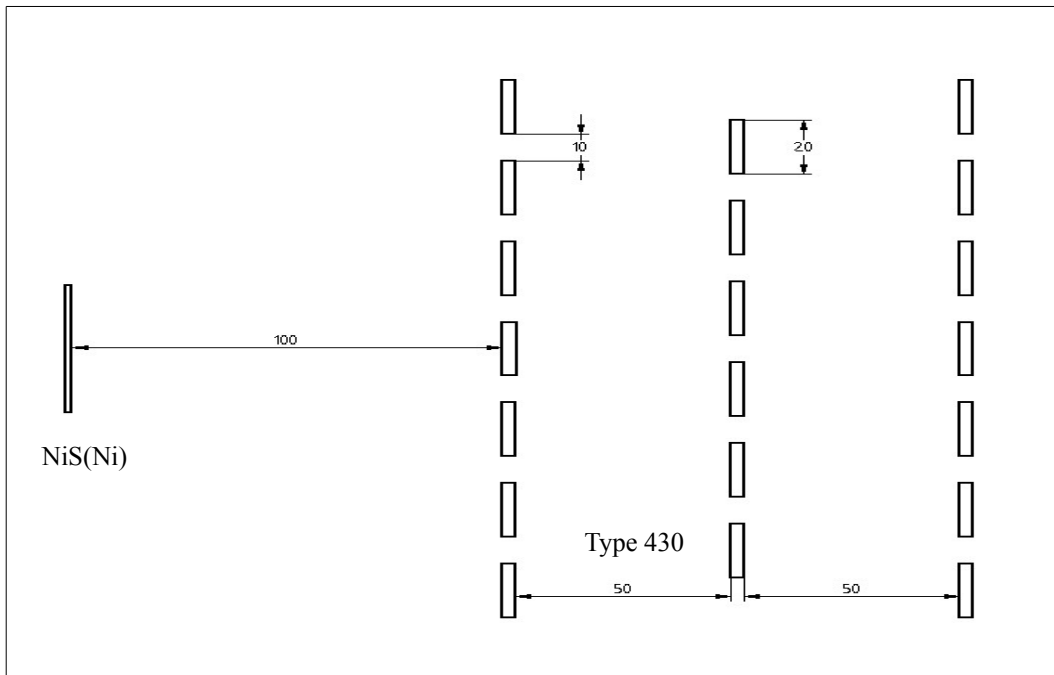


*Figure 15: Schematic of coupon placement in HDPE tank*

A Gamry Instruments PC4 Potentiostat/Galvanostat was used to measure the potential of the NiS(Ni) and a voltmeter was used to measure the potential on the face of the stainless steel coupons facing the NiS(Ni) electrode. Potential measurements were taken on the NiS(Ni) electrode and the stainless steel when the steel was first submerged and not connected to the NiS(Ni) electrode. The

stainless steel was then connected in series, the third row to the second row, the second row to the first row and then to the Ni electrode. Potential measurements were then taken at 1 h, 4 h, 10 h and 24 h intervals on the surface of the stainless steel coupons. This was repeated for each NiS(Ni) electrode having a surface area of 24 cm<sup>2</sup> using virgin acid, in order to get a 20:1 anode/cathode surface area ratio.

In order to determine the minimum surface area of NiS(Ni) to maintain passivity, another shielding experiment was conducted. The same stainless steel array was used, having exposed surface area of 472 cm<sup>2</sup> in a HDPE tank, containing 4L of virgin acid at room temperature. The array was coupled to NiS(Ni) of 24 cm<sup>2</sup> for 1 h in order to passivate it. Then part of the electrode was removed, reducing the surface area to 5 cm<sup>2</sup>, in order to get approximate 100:1 anode/cathode surface area ratio. Potential measurements were taken at 1 h, 4 h, 8 h, 24 h and 43 h on the surface of the stainless steel coupons using a voltmeter.

## **CHAPTER 4**

### **Results**

#### **Polarization Experiments**

##### *Cathodic Polarizations*

Cathodic polarizations were conducted on the NiS, NiS(Ni) and Pt electrodes at both room temperature and 60 °C. The NiS electrode was exposed for 1h in open circuit conditions in both cases before polarizations were conducted so that a steady open circuit potential could be established. The surface was visually inspected after each polarization and a slight greying of the surface was observed at both temperatures. The results of the cathodic polarization are show in Figure 16.

The open circuit potential of the NiS electrode was about 50 mV more positive at room temperature than at the elevated temperature. Both polarizations showed signs of mixed polarization, having both an activation controlled polarization at low overpotentials and showing the effects of concentration polarization at high overpotentials. In both cases, the polarization curves were relatively linear between 0 and  $-200 \text{ mV}_{\text{MSE}}$ , consistent with activation polarization. In addition, below  $-300 \text{ mV}_{\text{MSE}}$ , both polarizations appear to reach a limiting current density, approximately  $5.62 \times 10^{-3} \text{ A/cm}^2$  at room temperature and at  $15.8 \times 10^{-3} \text{ A/cm}^2$  at  $60^\circ\text{C}$ , a sign of concentration polarization. The increase in the limiting current is to be expected with the increase in temperature.

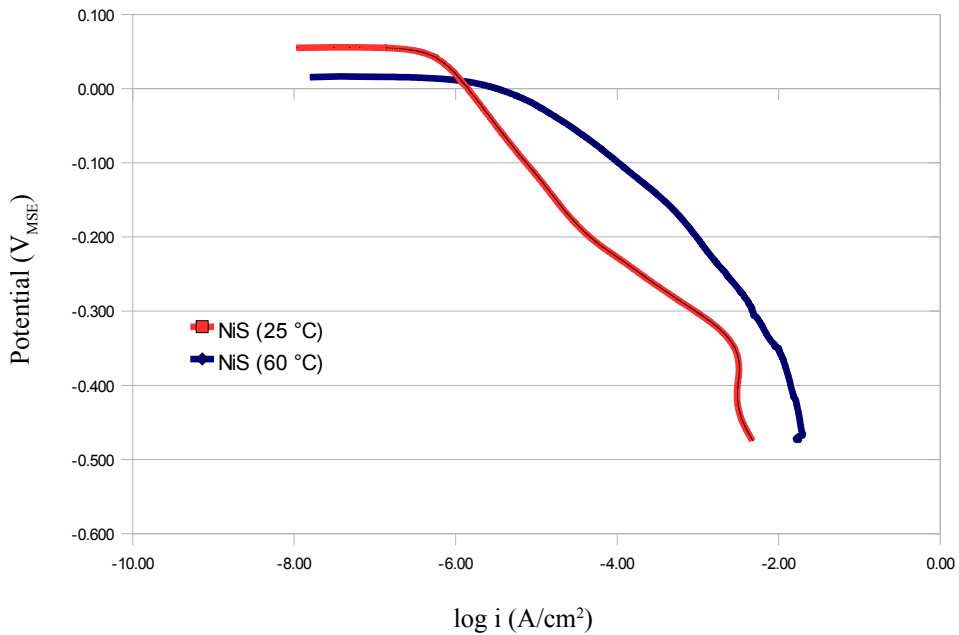


Figure 16: Cathodic polarizations of NiS at room temperature and  $60^\circ\text{C}$

The NiS(Ni) electrode was exposed for 3h and 1h at open circuit conditions at room temperature and 60 °C respectively, before polarizations were conducted so that a steady potential could be established. The surface was visually inspected after each polarization and was covered in a yellow film, that washed away during careful rinsing using anhydrous ethanol, C<sub>2</sub>H<sub>6</sub>O.

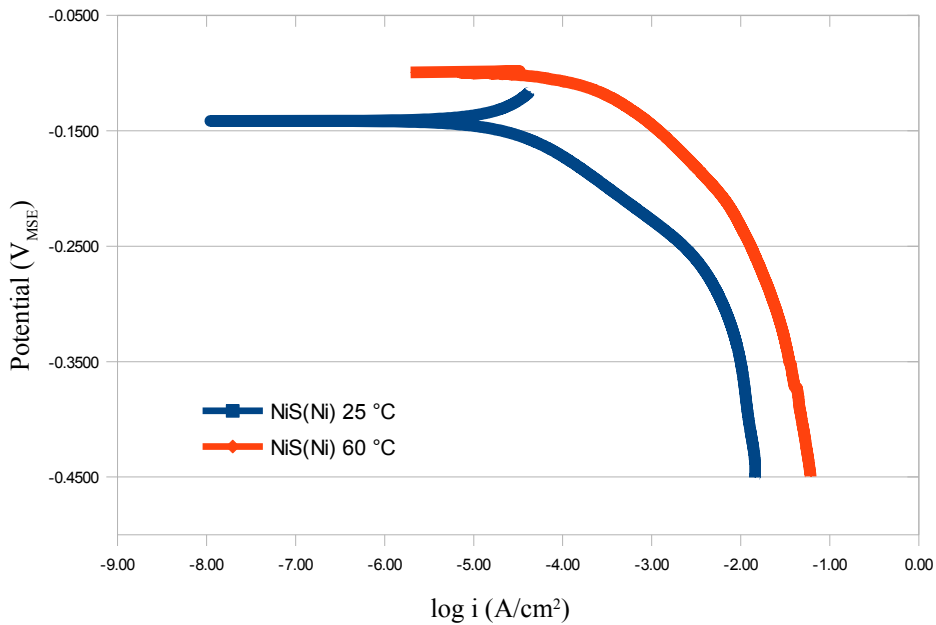


Figure 17: Cathodic polarization of NiS(Ni) at room temperature and 60 °C

The open circuit potential of the NiS electrode was about 10 mV more negative at the room temperature than at the elevated temperature. Both polarizations showed signs of mixed polarization, having both an activation controlled polarization at low overpotentials and showing the effects of

concentration polarization at higher overpotentials. In both cases, the polarization curves were relatively linear between  $-150 \text{ mV}_{\text{MSE}}$  and  $-300 \text{ mV}_{\text{MSE}}$ , consistent with activation polarization. In addition, below  $-300 \text{ mV}_{\text{MSE}}$ , both polarizations appear to reach a limiting current density, approximately  $1.77 \times 10^{-2} \text{ A/cm}^2$  at room temperature and  $6.3 \times 10^{-2} \text{ A/cm}^2$  at  $60 \text{ }^\circ\text{C}$ , a sign of concentration polarization. The increase in the limiting current is to be expected with the increase in temperature.

The Pt electrode was exposed in open circuit conditions at both temperatures before polarizations were conducted until a steady potential could be established. The surface was visually inspected after each polarization and showed no change.

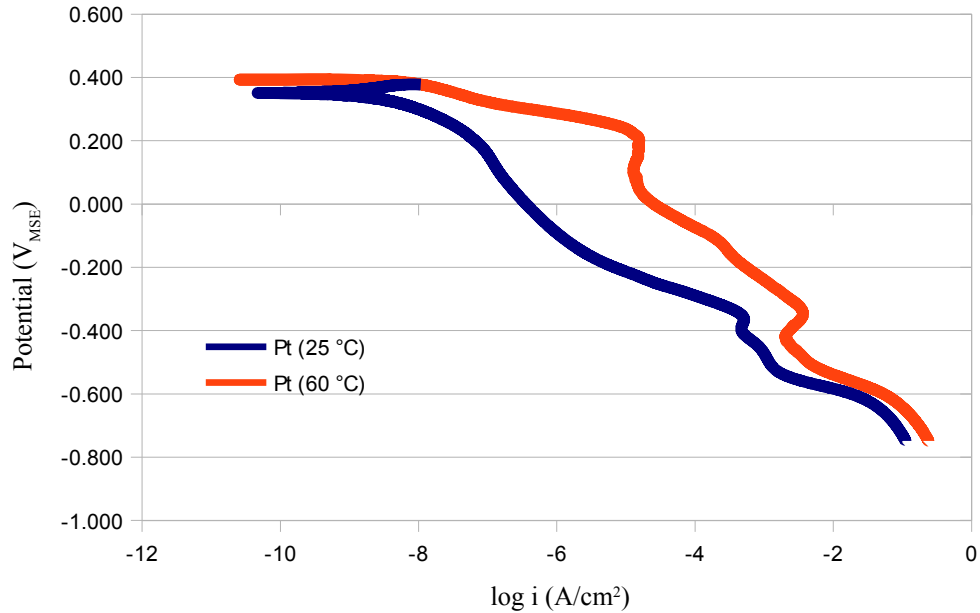
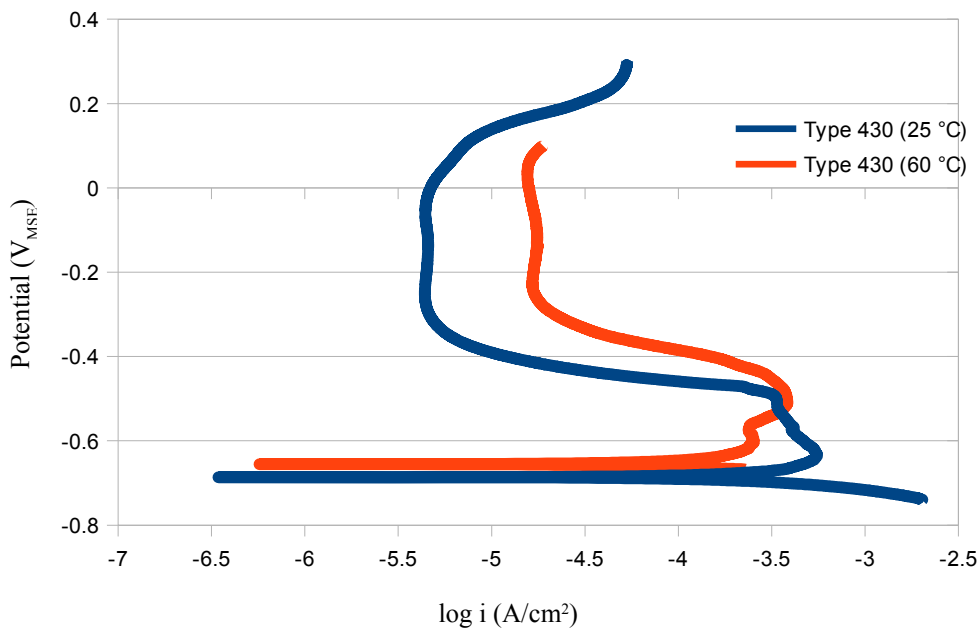


Figure 18: Cathodic polarization of Pt at room temperature and 60 °C

The open circuit potential was slightly more negative at the room temperature than at the elevated temperature. The polarization at the elevated temperature showed higher current densities at all potentials during the polarizations. Three distinct zones can be observed by the change in slopes during the polarizations, especially at the elevated temperature. These changes can be correlated to the different potential dependent cathodic reactions that occur on the surface of the platinum electrode [9].

### *Anodic Polarization*

The anodic polarization behaviour of Type 430 was characterized at room temperature and 60 °C. The electrodes were exposed for 1h in open circuit conditions until a steady potential was reached. The surface of the electrode was visually inspected after the polarization test and showed uniform corrosion on the surface.



*Figure 19: Anodic polarization of Type 430 at room temperature and 60 °C*

At both temperatures the Type 430 exhibited a passivation potential,  $E_p$ , at approximately -500 mV<sub>MSE</sub>. The  $i_{crit}$ , to achieve passivation was  $5.53 \times 10^{-4} A/cm^2$  at room temperature  $5.01 \times 10^{-4} A/cm^2$  at 60 °C . The passive current,  $i_p$ , needed to

maintain passivity was  $3.98 \times 10^{-6}$  A/cm<sup>2</sup> at room temperature and  $1.78 \times 10^{-5}$  A/cm<sup>2</sup> at 60 °C. The passivation range for the Type 430 at room temperature is approximately 500 mV, from -400 mV<sub>MSE</sub> to 100 mV<sub>MSE</sub>, while at 60 °C the range is approximately 400 mV, from -300 mV<sub>MSE</sub> to 100 mV<sub>MSE</sub>. The  $i_{crit}$  is not greatly effected by the increase in temperature, however, the passive region of the Type 430 is decreased by 100 mV and the passive current is increased by an order of magnitude at 60 °C.

## **Galvanic Couple Experiments**

### *NiS Surface Area Relationships*

The relative surface area of Type 430 to NiS needed to passivate the stainless steel was determined by conducting two galvanic coupling experiments at room temperature. Upon constructing an Evans diagram, shown in Figure 20, using the polarization data gathered at room temperature, surface ratios of Type 430 to NiS of 10:1 and 100:1 was chosen to test the passivation ability of the NiS electrode. These surface area ratios were chosen because the 10:1 ratio theoretically shows the optimal case for spontaneous passivation as the cathodic current density,  $i_c$ , is higher than the  $i_{crit}$  at  $E_{pp}$ . While the 100:1 ratio shows that the  $i_c$  is less than the  $i_{crit}$  required for passivation, and thus passivation is not expected in this case.

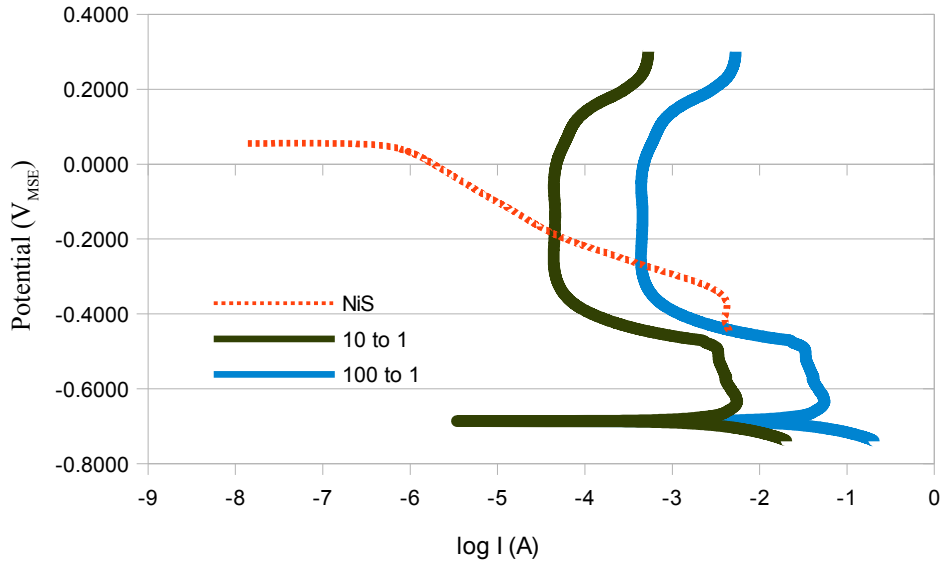
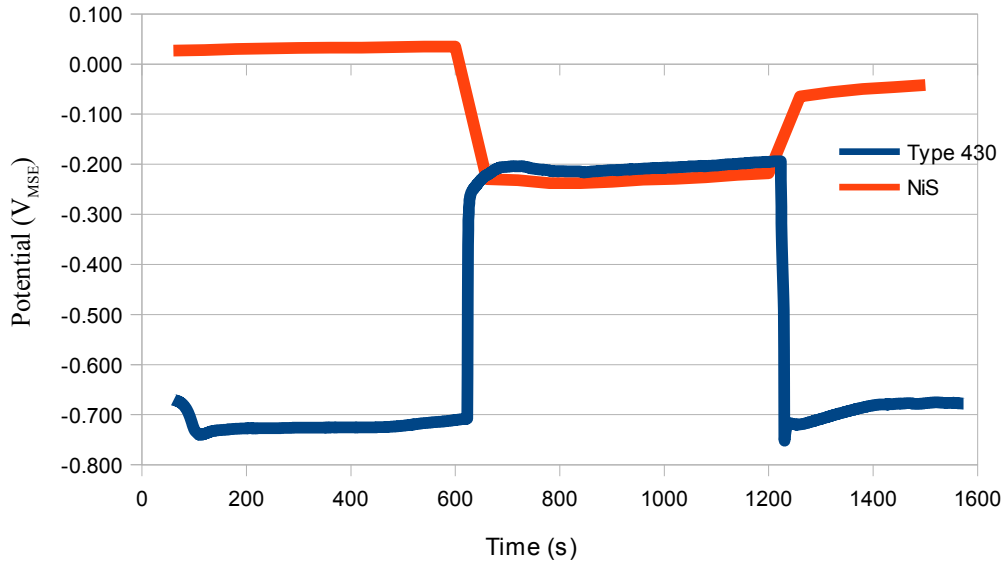
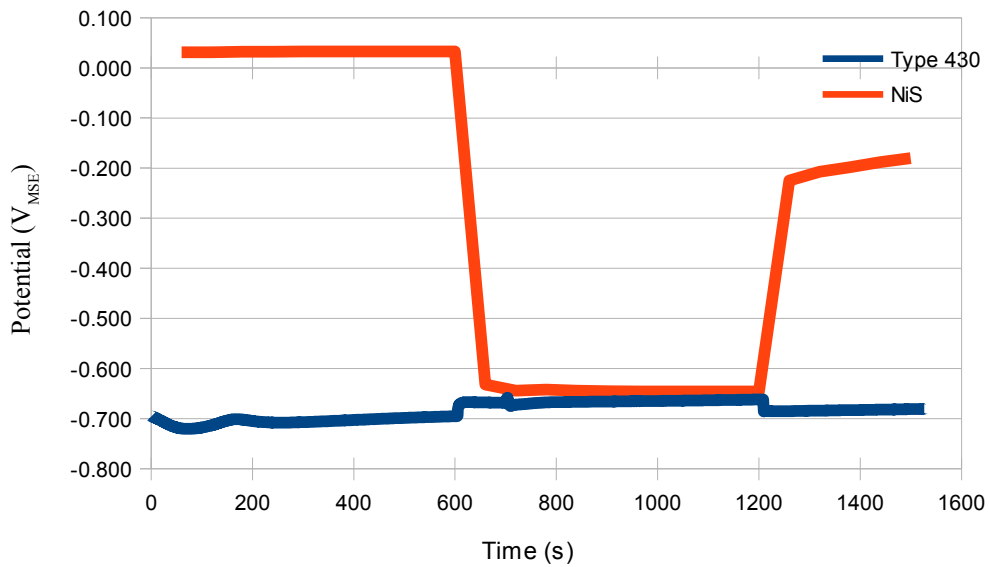


*Figure 20: Evans diagram showing the possible galvanic potential of Type 430 : NiS surface area ratios*

The NiS electrode of  $0.75 \text{ cm}^2$  was coupled to two suspended Type 430 stainless steel electrodes of  $7.5 \text{ cm}^2$  and  $75 \text{ cm}^2$ , giving a surface area ratio of 10:1 and 100:1 respectively. The system was exposed to the room temperature 93.5 wt %  $\text{H}_2\text{SO}_4$  for 1 h uncoupled. Data was then recorded for 600 s in the uncoupled state, 300 s coupled and 300 s uncoupled. The results of these experiments are shown in Figure 21.



a)



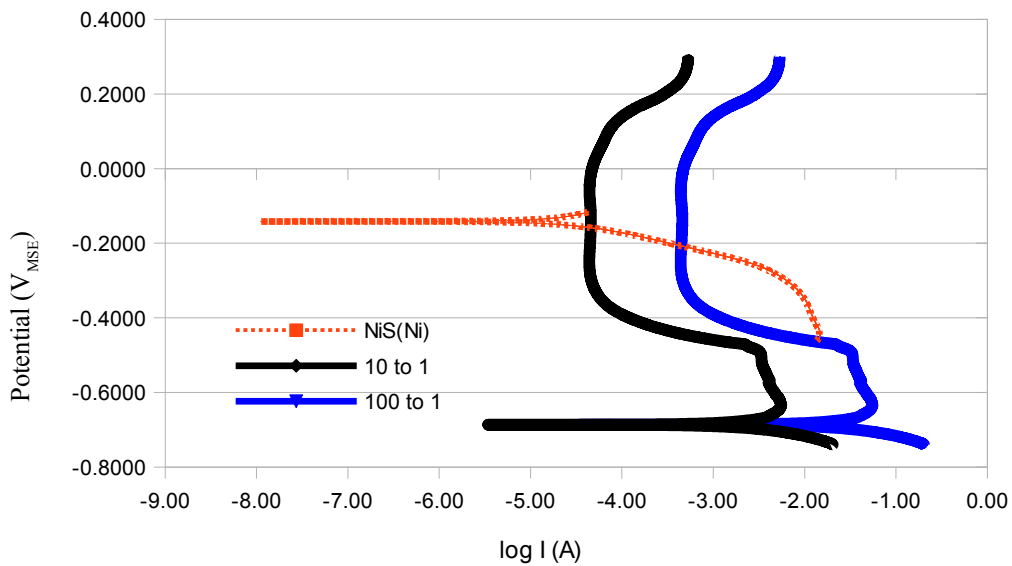
(b)

Figure 21: Potential on NiS and 430 surface during galvanic couple experiment; a) 10:1 (SS:NiS) ratio b) 100:1 (SS:NiS) ratio

Both experiments showed that the Type 430 electrode corroded actively at approximately  $-700 \text{ mV}_{\text{MSE}}$  before being coupled to the NiS electrode, while the NiS electrode maintain a uncoupled potential of about  $30 \text{ mV}_{\text{MSE}}$ . Bubbles were seen evolving on the surface of the stainless steel electrodes during this time. When coupled to the NiS electrode, the suspended Type 430 electrode having the 10:1 surface area ratio to the NiS was passivated, the potential on the surface quickly reaching a steady potential of  $-200 \text{ mV}_{\text{MSE}}$ , well within the passive range of the stainless steel, shown in Figure 19, and the evolution of bubbles on the surface of the stainless steel also stopped. The effect of the galvanic coupling also reduced the potential of the NiS electrode to similar potential, about  $-240 \text{ mV}_{\text{MSE}}$ , which is approximately what was expected from the Evans diagram shown in Figure 20. The suspended Type 430 stainless steel electrode having the 100:1 surface area ratio did not passivate when coupled to the NiS electrode, the potential was maintained at  $-650 \text{ mV}_{\text{MSE}}$  and the evolution of bubbles on the surface of the stainless steel continued. The effect of the galvanic coupling also reduced the potential of the NiS electrode to similar potential, about  $-645 \text{ mV}_{\text{MSE}}$ . Upon decoupling, both systems showed a quick return to their separate uncoupled potential. Therefore the experiments were consistent with the predictions from the constructed Evans diagram, shown in Figure 20.

### *NiS(Ni) Surface Area Relationships*

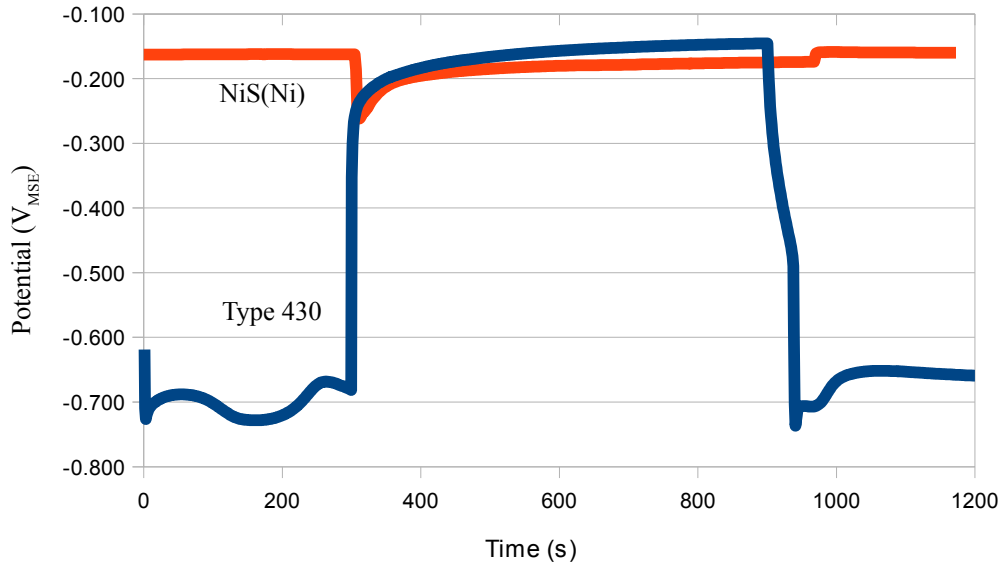
A similar set of experiments were conducted to determine the relative surface area of Type 430 to NiS(Ni) needed to passivate the stainless steel. Upon constructing another Evans diagram, shown in Figure 22, using the polarization data gathered at room temperature previously, similar surface ratios of stainless steel to NiS(Ni) of 10:1 and 100:1 was also chosen to test the passivation ability of the NiS(Ni) electrode.



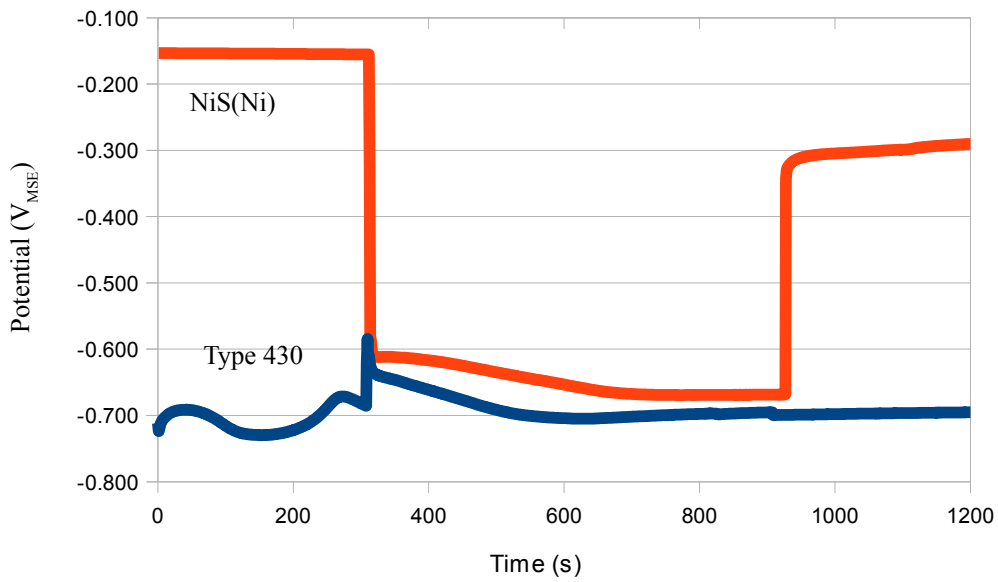
*Figure 22: Evans diagram showing the possible galvanic potential of both Type 430: NiS(Ni) surface area ratios*

A NiS(Ni) electrode of 1 cm<sup>2</sup> was coupled to two suspended stainless steel electrodes of 10 cm<sup>2</sup> and 100 cm<sup>2</sup>, giving a surface area ratio of 10:1 and 100:1

respectively. The system was exposed to the room temperature 93.5 wt% H<sub>2</sub>SO<sub>4</sub> for 1 h uncoupled. Data was then recorded for 300 s in the uncoupled state, 600 s coupled and 300 s uncoupled. The results of these experiments are shown in Figure 23.



(a)



(b)

Figure 23: Potential on NiS and Type 430 surface during galvanic couple experiment; a) 10:1 (SS:NiS(Ni)) ratio b) 100:1 (SS:NiS(Ni)) ratio

Both systems showed that the suspended Type 430 electrode corroded actively at approximately  $-700 \text{ mV}_{\text{MSE}}$  before being coupled to the NiS(Ni) electrode, while the NiS(Ni) electrode maintain a potential of about  $-150 \text{ mV}_{\text{MSE}}$ . Bubbles were also seen evolving on the surface of the stainless steel electrodes during this time. When coupled to the NiS(Ni) electrode, the stainless steel electrode having the 10:1 surface area ratio to the NiS(Ni) was passivated, the potential on the surface quickly reaching a steady potential of  $-200 \text{ mV}_{\text{MSE}}$  and the evolution of bubbles on the surface of the stainless steel stopped. The effect of the galvanic coupling also slightly reduced the potential of the NiS(Ni) electrode to about  $-200 \text{ mV}_{\text{MSE}}$ . The stainless steel electrode having the 100:1 surface area ratio to the NiS(Ni) was not passivated when coupled to the NiS(Ni) electrode, the potential on the surface maintain a potential of  $-700 \text{ mV}_{\text{MSE}}$  and the evolution of bubbles on the surface of the stainless steel continued. The effect of the galvanic coupling also reduced the potential of the NiS electrode to similar potential, about  $-645 \text{ mV}_{\text{MSE}}$ . Upon decoupling in the 10:1 surface area case, the NiS(Ni) potential rose quickly back to its corrosion potential, while in the 100:1 case, the potential rose only to  $-300 \text{ mV}_{\text{MSE}}$  but was gradually increased. Upon decoupling the stainless steel surface continued to corrode in the active state. Again, these findings are consistent with the prediction from the constructed Evans diagram, shown in Figure 23.

## **Shielding Experiments**

An Evans diagram was constructed, shown in Figure 24, to determine the minimum surface area ratio needed to passivate the Type 430 array using a NiS(Ni) electrode, as well as to determine the surface area ratio needed to maintain passivation. A surface area ratio of 10:1 was chosen since theoretically it would provide enough current to passivate the stainless steel array. A ratio of 20:1 was chosen as it could theoretically exhibit active – passive transitional behaviour. While a 100:1 ratio was chosen to determine whether the array could maintain passivity once the system was already passivated using a larger suspended NiS(Ni) electrode, using a stainless steel to NiS(Ni) surface area ratio of 20:1. This 100:1 ratio was used to determine whether such a large surface ratio could provide enough current to maintain the current needed for passivation,  $I_p$ .

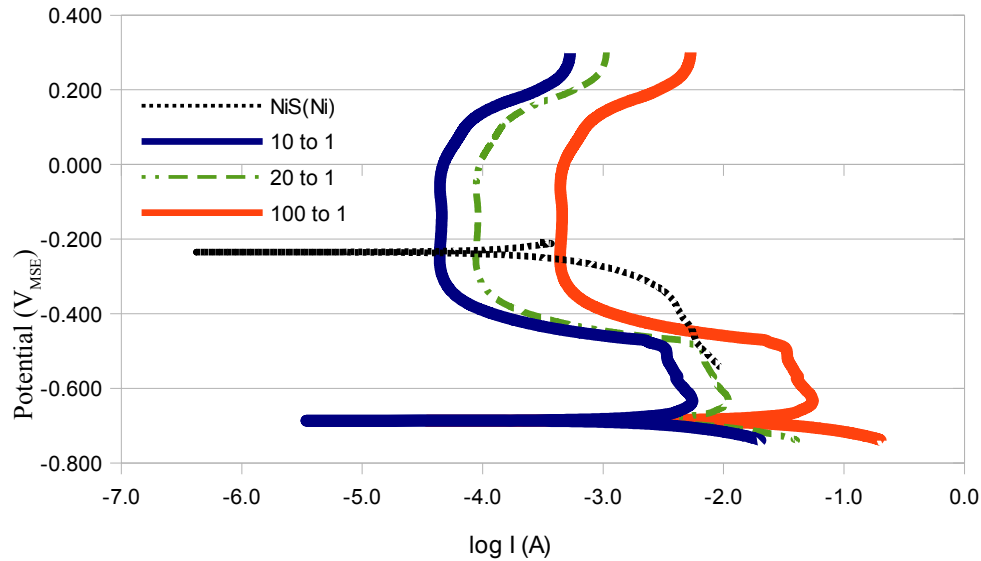
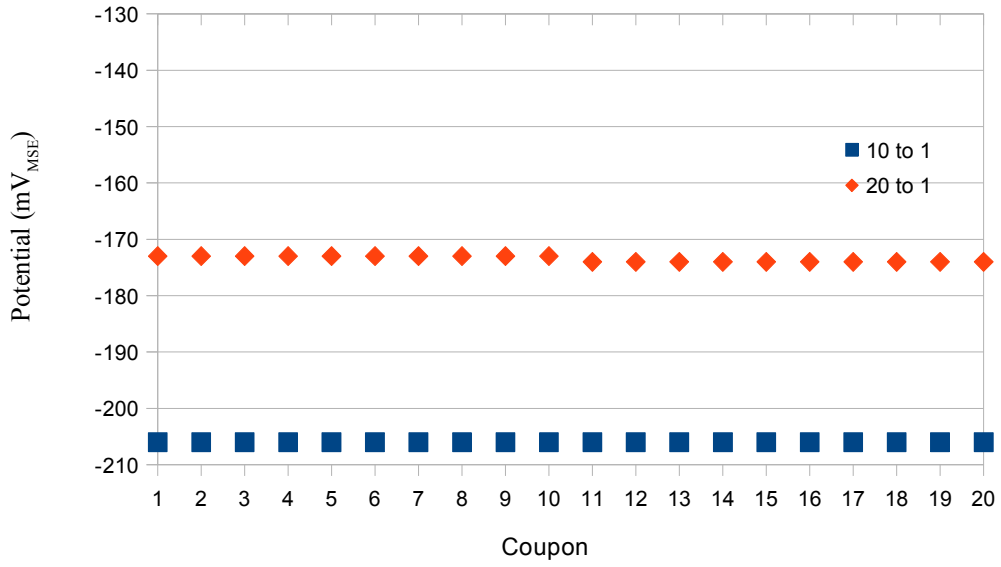


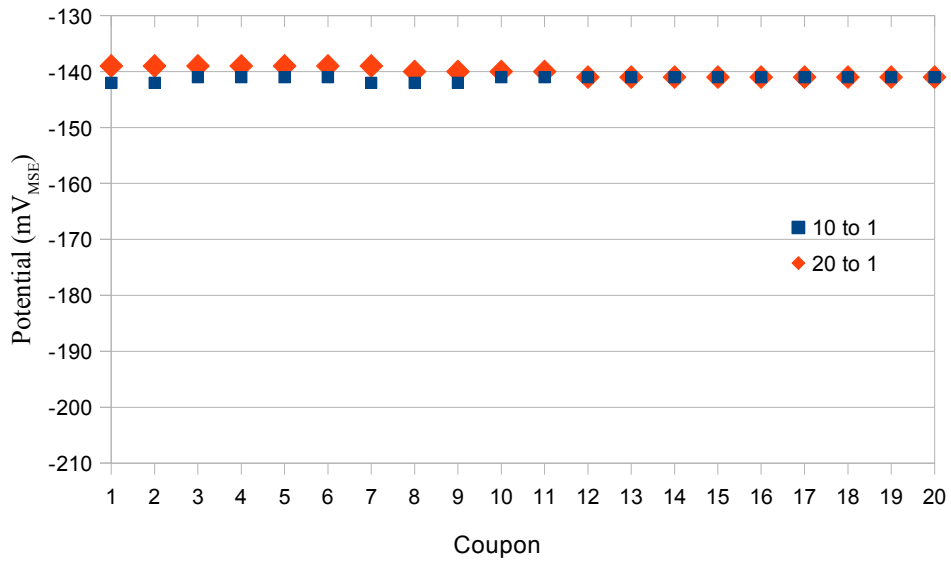
Figure 24: Evans diagram showing the possible galvanic potential of three Type 430 : NiS(Ni) surface area ratios

The 10:1 and 20:1 surface area ratios showed a similar behaviour when coupled together; both were able to passivate the stainless steel array and maintain this passivity for 24 h. When uncoupled, the stainless steel array corroded actively; bubbles evolved on the surface and the array maintained a corrosion potential of about  $-715 \text{ mV}_{\text{MSE}}$ . When coupled together, the potentials on the surface of the stainless steel coupons reached a minimum after 1 h of exposure. This is because at this time the NiS film is still growing on the Ni surface, which at room temperature takes 3 h to form. The potentials slowly increased in both systems as the exposure continued up to 10 h as the NiS film on the Ni substrate

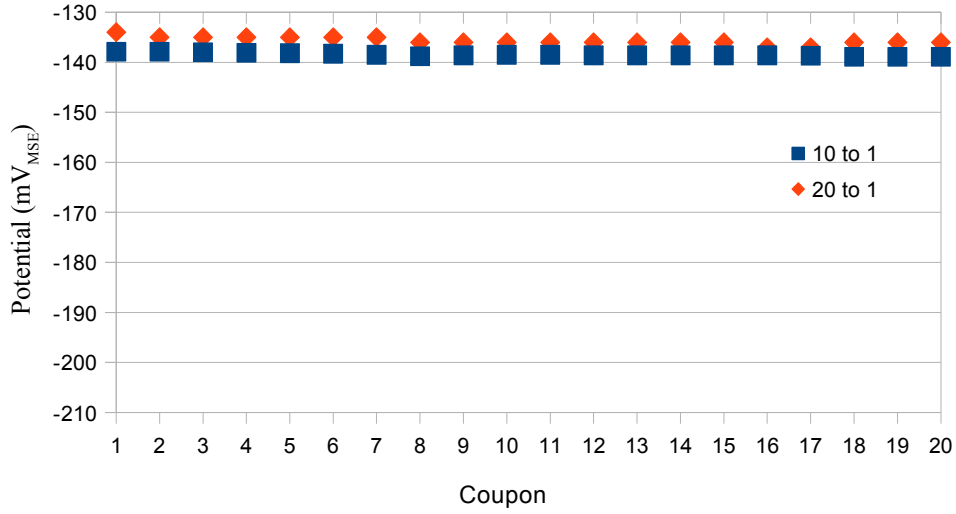
stabilizes. However, potentials over the entire array of both systems were slightly lower after 24 h than 10 h, as the NiS film starts to degrade or spall off. Both systems also show no shielding effects as there was very little variance in the potential along the three rows of the array. Evidence of this can be seen in Figure 25.



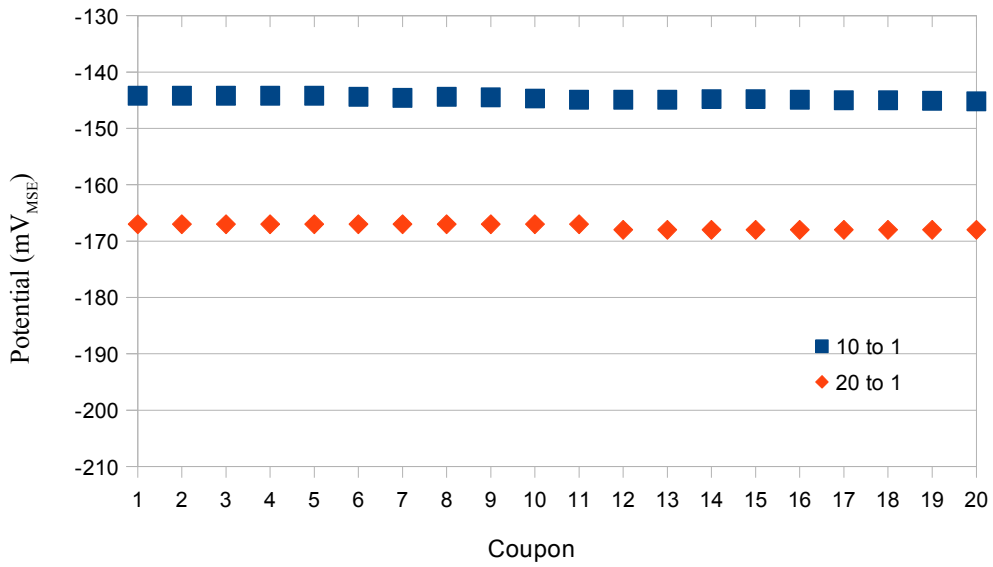
(a)



(b)



(c)



(d)

Figure 25: Potentials on Stainless Steel coupons for 10:1 and 20:1 surface area ratios; (a) 1 h (b) 4 h (c) 10 h (d) 24 h

In order to test whether a surface area ratio of 100:1 of stainless steel to NiS(Ni) can maintain passivation across the entire stainless steel array, an experiment was conducted. First, it was shown that a 100:1 surface area ratio that could not passivate the array, as shown in Figure 26. The array was then passivated using a NiS(Ni) electrode having a 20:1 surface area ratio.

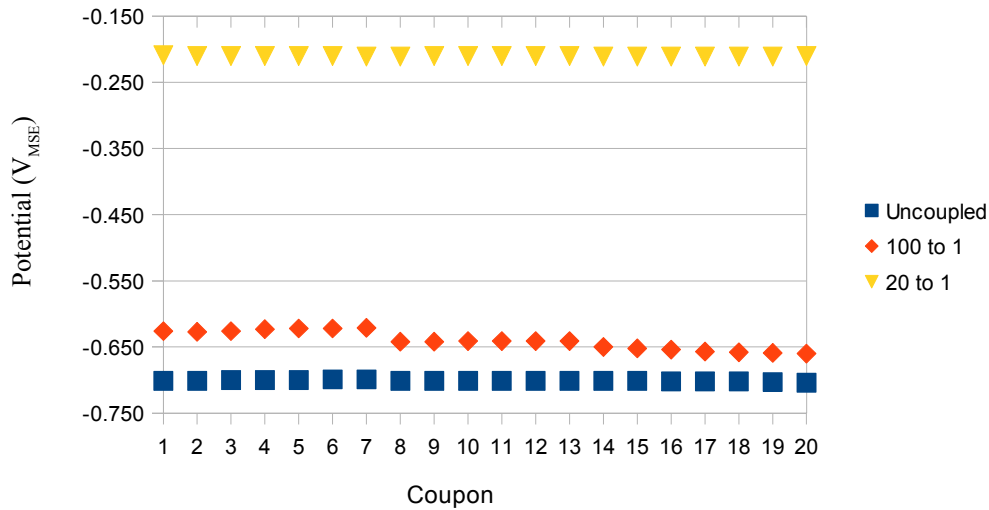


Figure 26: Potentials of array when uncoupled, coupled to 100 to 1 and then 20 to 1 surface area ratios

Once passivity had been established and maintained, part of the electrode was removed, exposing only an area equivalent to a 100:1 surface area ratio. This electrode was able to maintain passivity for 43 h at room temperature. After that

the stainless steel array began to actively corrode at a potential of -650 mV, showing a breakdown in passivity.

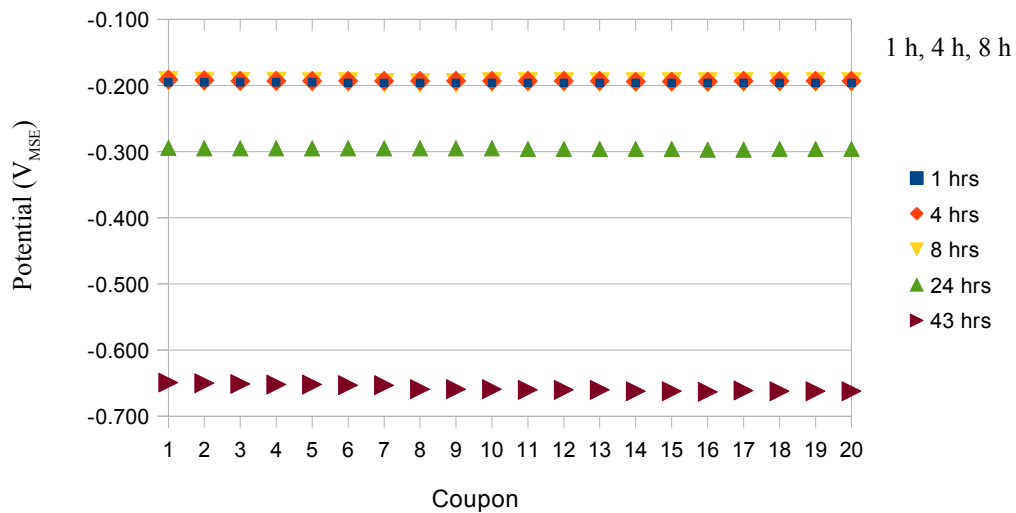


Figure 27: Potential on Type 430 array when coupled to 100 to 1 surface area ratio

The potential on the surface of the array was relatively stable for the first 8 h of exposure, and then slowly started to decrease, as the NiS film starts to degrade. The system could not maintain passivity after 43 h, and the array starts to corrode rapidly in its active state as evidenced by the bubbles seen evolving on the surface of the stainless steel coupons.

## **CHAPTER 5**

### **Discussion**

When considering what materials can be used as a cathode in a concentrated  $\text{H}_2\text{SO}_4$  – stainless steel GCAP system, the material must exhibit a number of key attributes. The cathode must be able to generate the  $I_{\text{crit}}$  needed to passivate and maintain the passivity of the stainless steel in such a GCAP system. The anode/cathode surface area ratios needed to protect the stainless steel must be high enough to make such a system practical. It must also be stable when exposed to concentrated  $\text{H}_2\text{SO}_4$ , that is, the cathode must not readily react with the acid and it must be able to maintain its stability in the acid for extended periods of time. The corrosion potential of the cathode should be less than the transpassive potential of the stainless steel in order to eliminate transpassivation as an issue. The cathode should have a high electric conductivity to ensure that reaction rates along the surface for the cathode is consistent and also not contribute greatly to the overall circuit resistance.

### **Ability to Initiate Passivity**

Pt is frequently used as an electrode material in electrochemical cells and is recognized as a one of the best electrocatalysts found in nature. This is largely due to its electrochemical stability; dissolution of Pt only occurring at highly anodic potentials,  $-1.118 \text{ V}_{\text{SHE}}$ . Thus, platinum is often used as reference electrodes in ICAP systems used to protected  $\text{H}_2\text{SO}_4$  - stainless steel systems [1,3,4-5]. Bianchi et al. [48] and Nakahara et al. [49] showed that Pt electrodes were able to generate the current densities needed to protect Type 304 and Type 316 stainless steels when galvanically coupled at a variety of temperatures and acid concentrations. Thus, Pt is a appropriate material to compare against the NiS and NiS(Ni) to determine their effectiveness as a cathode material for a GCAP system. Figure 28 shows an Evans diagram of the cathodic polarization behaviour of Pt, NiS and NiS(Ni) and the anodic polarization behaviour of Type 430 stainless steel normalized for an area of  $1 \text{ cm}^2$  at room temperature in quiet 93.5 wt %  $\text{H}_2\text{SO}_4$ .

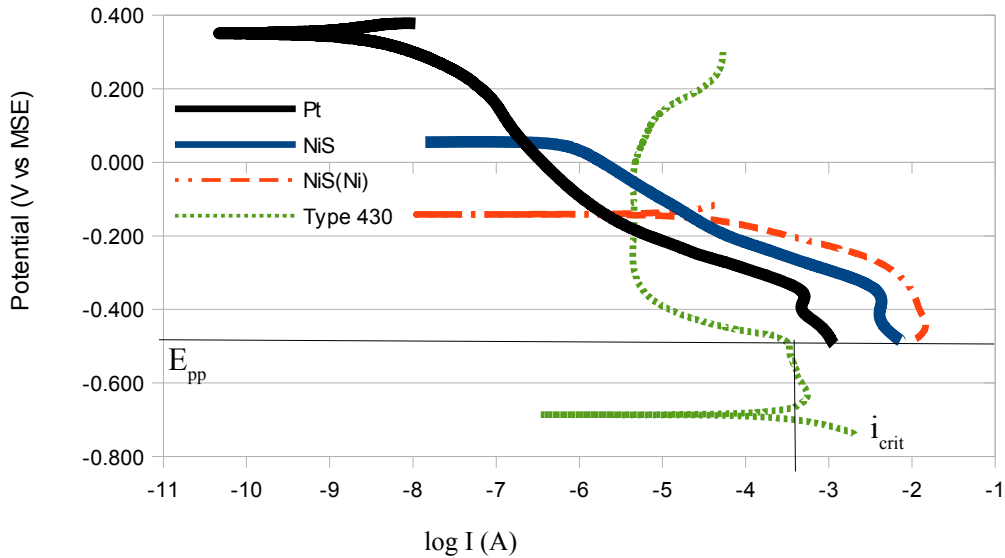


Figure 28: Evans diagram of polarization behaviour of cathode and anode materials at room temperature in quiet 93.5 wt%  $H_2SO_4$

A comparison of the current densities of the three prospective cathode materials at the passivation potential,  $E_{pp}$ , of the Type 430 stainless steel shows that all three cathode materials are able to provide current densities greater than the  $i_{crit}$ ,  $3.16 \times 10^{-4} \text{ A/cm}^2$ , needed to passivate the stainless steel. NiS(Ni) provided the greatest current density at  $E_{pp}$ , approximately  $0.011 \text{ A/cm}^2$ , followed by NiS,  $7.94 \times 10^{-3} \text{ A/cm}^2$ , while the Pt electrode provided the lowest current density,  $1.12 \times 10^{-3} \text{ A/cm}^2$ . NiS and NiS(Ni) were able to generate similar current densities at  $E_{pp}$  differing by only  $3.06 \times 10^{-3} \text{ A/cm}^2$ , while there is an order of magnitude

difference between the current density generated by Pt and NiS(Ni) at  $E_{pp}$ . The NiS and NiS(Ni) electrodes are able to provide current densities approximately 2 orders of magnitude greater than the critical current density required by Type 430 stainless steel for passivation in a 1:1 surface area ratio.

Similar observations and behaviours can be seen at elevated temperatures, 60 °C, for the anode and cathode materials. Figure 29. shows an Evans diagram of cathodic behaviour of Pt, NiS and NiS(Ni) and the anodic polarization behaviour of Type 430 stainless steel normalized for an area of 1cm<sup>2</sup> at 60 °C in quiet 93.5 wt% H<sub>2</sub>SO<sub>4</sub>.

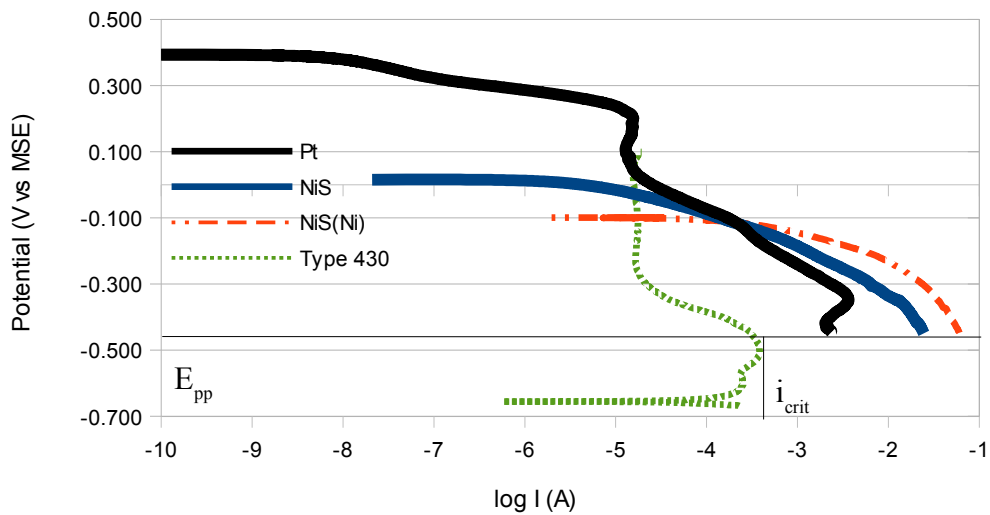


Figure 29: Evans diagram of polarization behaviour of cathode and anode materials 60 °C in quiet 93.5 wt% H<sub>2</sub>SO<sub>4</sub>

A comparison of the current densities of the three prospective cathode materials at the passivation potential,  $E_{pp}$ , of the Type 430 stainless steel shows that all the cathode materials are able to provide current densities greater than the  $i_{crit}$ ,  $3.98 \times 10^{-4} \text{ A/cm}^2$  needed to passivate the stainless steel. NiS(Ni) provided the greatest current density, approximately  $0.06 \text{ A/cm}^2$ , followed by NiS,  $0.025 \text{ A/cm}^2$ , while the Pt electrode provided a current density of  $2.51 \times 10^{-3} \text{ A/cm}^2$ . The NiS and NiS(Ni) electrodes generate current densities of the same magnitude while the current generated by the Pt is a magnitude smaller. Similar to the results found at room temperature, the difference in current generated by the NiS and NiS(Ni) electrodes is two orders of magnitude greater than the  $i_{crit}$  required of the passivation of Type 430 stainless steel in a 1:1 surface area ratio. The NiS and NiS(Ni) electrodes are able to provide the necessary current, up two orders of magnitude greater than the  $i_{crit}$  needed for passivation, to passivate Type 430 stainless steel at both temperatures; room temperature and  $60 \text{ }^\circ\text{C}$ . In comparison to Pt, these electrodes are able to provide current densities one order of magnitude greater than Pt at both temperatures at the passivation potential,  $E_{pp}$ , of the Type 430 stainless steel.

### **Surface Area Ratios**

The large difference between the  $i_{crit}$  needed for passivation and the current generated by the NiS and NiS(Ni) electrodes in a 1:1 surface area ratio would

allow for a significant increase in surface area of the stainless steel before the NiS and NiS(Ni) electrodes of the same size would not be able to provide the current needed to passivate the stainless steel. This is an important factor when considering a cathode materials for GCAP system. While GCAP systems have the advantage of not needing an external current to passivate the anode, a low anode/cathode surface area could make the use of such a system impractical in an industrial setting.

Two surface area experiments were conducted with NiS and NiS(Ni) electrodes coupled to Type 430 electrodes at room temperature to determine the anode/cathode ratio needed to protect the stainless steel. These experiments showed that both electrodes were able to passivate the stainless steel when coupled in a 10:1 anode/cathode surface area relationship, while the cathode was unable to generate the  $i_{crit}$  needed to passivate the stainless steel when coupled in a 100:1 anode/cathode ratio. In addition, NiS(Ni) electrodes were galvanically coupled to a stainless steel array having an anode/cathode ratio of 20:1 and successfully passivated it. Another experiment was conducted showing that when passivated, a anode/cathode surface area of 100:1 was able to maintain passivity for over 24 h. The combination of the surface area and galvanic couple experiments lead to the following conclusions; NiS and NiS(Ni) electrodes are able to provide the  $i_{crit}$  needed to passivate Type 430 at anode/cathode ratios of

10:1, while NiS(Ni) electrodes were able to provide the  $i_{\text{crit}}$  needed to passivate the Type 430 at a ratio of 20:1. In addition it was shown that the NiS(Ni) electrode was able to maintain passivity of the Type 430 array using a surface area ratio of 100:1. Theoretically, since NiS(Ni) and NiS showed similar cathodic polarization behaviour, a similar performance is expected from a monolithic NiS electrode.

Nakahara et al. [49] showed that Type 316 coupled to Pt at a surface ratio of 150:1 in 100 wt% H<sub>2</sub>SO<sub>4</sub> in a laboratory test was able to passivate the stainless steel, and this was used as the basis to implement Au plated Type 316 electrodes at the same ratio in an industrial capacity. This example for literature is the best benchmark to compare the results of the experiments conducted with the NiS and NiS(Ni) electrodes. While Bianchi et al. [48] showed anode/cathode ratios of 1:5 were needed in order to passivate Type 304 at 25 °C in 12.5 M (75 wt%) H<sub>2</sub>SO<sub>4</sub> using Pt as the cathode, the acid used in their experiment was a weaker oxidizer, due to the increased amount of the H<sub>2</sub>O in H<sub>2</sub>SO<sub>4</sub> solution when compared the acid used in these experiments. Zhong et al. [50] showed their PANI electrode to be able to passivate 1Cr13 exposed to 38 wt% H<sub>2</sub>SO<sub>4</sub> at 25 °C using a 1:1 anode/cathode surface area ratio. Again, the acid used was of a much different concentration. Thus Nakahara et al. [49] experiment gives the best indicator as to what anode/cathode surface area ratios would be viable for a GCAP system consisting of stainless steel and concentrated H<sub>2</sub>SO<sub>4</sub>.

*Table 7: Summary of GCAP systems and the surface area ratios needed for passivation*

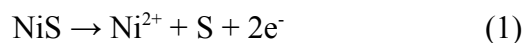
<b>Anode Material</b>	<b>Cathode Material</b>	<b>Acid concentration</b>	<b>Surface area needed to passivate</b>
Type 316[49]	Pt/Au	100 wt%	150 to 1
Type 304[48]	Pt	75 wt%	1 to 5
1Cr13[50]	PANI	38 wt%	1 to 1

On first view it would seem, NiS and NiS(Ni) have relatively poor performance when compared to the Pt and Au plated electrodes used by Nakahara et al., requiring at least six times the amount of NiS or NiS(Ni) surface area to passivate the stainless steel. However, the main difference between Nakahara et al. experiment and this one is the alloys used, Type 430 in this case and Type 316 in the Nakahara et al. experiment. Type 316 as well as other nickel containing stainless steels such as Type 316, 316L and 304 have shown to show potential oscillations, active-passive spikes, when immersed in concentrated H<sub>2</sub>SO<sub>4</sub>, 95 – 100 wt% [9-10, 28-29]. Thus in Nakahara et al. experiment's case, the Type 316 would undergo periodic passivisation without the use of the galvanic couple, and the effect of the galvanic coupling to Pt or Au electrodes is to simply maintain passivity, that is to prevent potential spikes into the active region of the stainless steel. The galvanic couple experiments using NiS(Ni) have shown that an anode/cathode surface area ratio of 100:1 was able to maintain passivity of an already passivated Type 430 array for more than 24 h. This surface area ratio is

more in line with the 150:1 anode/cathode ratio used by Nakahara et al. in their industrial operation.

### **Maintaining Passivity**

The NiS(Ni) electrode was only able to maintain passivity for 24 h, which is considered unacceptable performance for an industrial setting. The NiS(Ni) electrode has a very thin NiS film formed in situ on the nickel substrate, and, thus the long term stability of NiS(Ni) electrodes is very poor, such electrodes only lasting 30 h at room temperature and less than 8 h at 60 °C. From Figure 29. it is observed that Pt had the highest open circuit potential at 0.35 V<sub>MSE</sub> followed by the open circuit potential of NiS at 0.05 V<sub>MSE</sub> and NiS(Ni) had the lowest open circuit potential at -0.15 V<sub>MSE</sub> at room temperature. Since Pt is inert when exposed to concentrated H<sub>2</sub>SO<sub>4</sub>, the difference between its open circuit potential and the corrosion potential of the NiS indicates that the NiS corrodes when exposed to concentrated H<sub>2</sub>SO<sub>4</sub>. If the NiS was an inert electrocatalyst, one would expect a corrosion potential closer to that of the open circuit potential of the Pt. Kish [9] proposed that the anodic dissolution of the NiS occurs at a significant rate along with the cathodic process on the NiS according to the following reaction which has a reversible potential of 0.162 V<sub>SHE</sub>.



The difference between the potentials of the NiS and NiS(Ni) samples can be

attributed the fact that the NiS(Ni) itself is a galvanic couple between the base Ni substrate and the NiS film, and, thus its mixed potential should fall between the corrosion potential of NiS and that of pure Ni. The corrosion of the thin NiS film on the nickel substrate was the rationale behind the development of a monolithic NiS electrode.

A monolithic NiS electrode would be able to maintain passivity longer than a NiS(Ni) electrode, as it is not limited to the thickness of the film formed on the Ni substrate. However, it still corrodes when exposed to concentrated H<sub>2</sub>SO<sub>4</sub>. An estimated corrosion rate of the NiS electrode at open circuit conditions can be determined by finding the corrosion current density,  $i_{\text{corr}}$ , of the electrode via Tafel extrapolation using the cathodic polarizations at room temperature and 60 °C. Shown in Figure 30. is the cathodic polarization behavior of NiS at room temperature and 60 °C, as well as their respective  $i_{\text{corr}}$ , found using Tafel extrapolation.

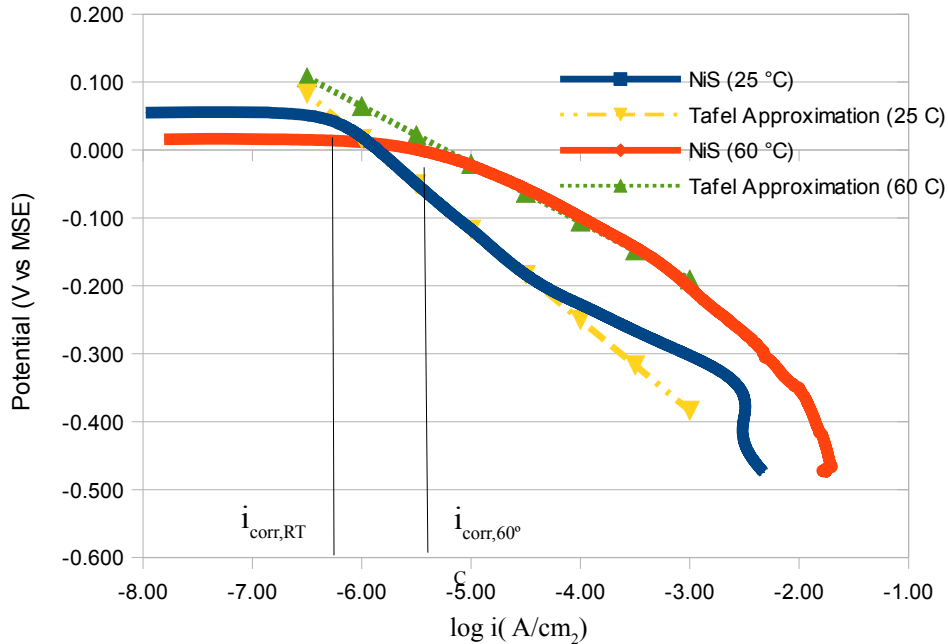


Figure 30: Determination of corrosion current densities of electrodes using Tafel extrapolation

The  $i_{\text{corr}}$  of the NiS electrode at room temperature was  $5.59 \times 10^{-7}$ , while at 60 °C it was  $5.01 \times 10^{-6}$ . Using this data as well as the equation,

$$r = 0.00327 \frac{ai}{nD}$$

where  $a$  is the atomic weight (g/mol) of NiS,  $i$  the current density ( $\text{A}/\text{cm}^2$ ),  $n$  the number of equivalents exchanged and  $D$  the density ( $\text{g}/\text{cm}^3$ ) of NiS, the estimated corrosion rate,  $r$  in mm/yr, of the NiS electrode can be calculated. The corrosion rates were found to be 0.014 mm/yr at room temperature and 0.128 mm/yr at 60 °C. On nickel substrates, the NiS film observed to be stable for over 125 h and 30 h, in quiet 93.5 wt%  $\text{H}_2\text{SO}_4$  at room temperature and 60°C respectively. FIB milling of NiS(Ni) electrodes have shown that the film itself is approximately 200

– 400 nm at 60 °C [64]. Given the estimated corrosion rates and the film thickness, the NiS film is estimated should be stable at 60 °C for 13 to 27 h, which is inline with observed data.

The surface area experiments have shown that a surface area ratio of 100:1 was enough to maintain passivity of Type 430 stainless steel. However, due to the nature of the NiS film formed on the NiS(Ni) electrodes, the passivity could not be maintained for extended periods of time. In theory, a monolithic NiS electrode would be able to provide the current needed to maintain passivity as it corrodes until it is unable to generate the current needed due to the reduction in surface area caused by its corrosion. A minimum surface area ratio needed to maintain passivity at room temperature can be estimated and is shown on the Evans diagram shown in Figure 31. A surface area ratio of 500:1 at room temperature was estimated to be the largest surface area ratio that would allow the NiS electrode to generate the current needed to maintain passivity. Using this information and the corrosion rates, one can estimate the lifetime of a monolithic NiS electrode. For example, if an austenitic stainless steel cylindrical tank having an area of 1000 cm<sup>2</sup> was to be protected, an initial NiS electrode of 10 cm<sup>2</sup> would be able to generate the current needed to maintain passivity. Assuming that the electrode only corrodes radially and that the length of the tank is much greater than the radius of the tank, theoretically a NiS electrode having a surface area of 2 cm<sup>2</sup>

would be able to maintain the passivity of the tank. At room temperature the reduction from 10 cm<sup>2</sup> to 2 cm<sup>2</sup> would take 704 yr and at 60°C it would take 77 yr. Though NiS is not inert in concentrated H<sub>2</sub>SO<sub>4</sub>, its corrosion rate is relatively low, and, therefore it would be able to maintain its stability in the acid for extended periods of time.

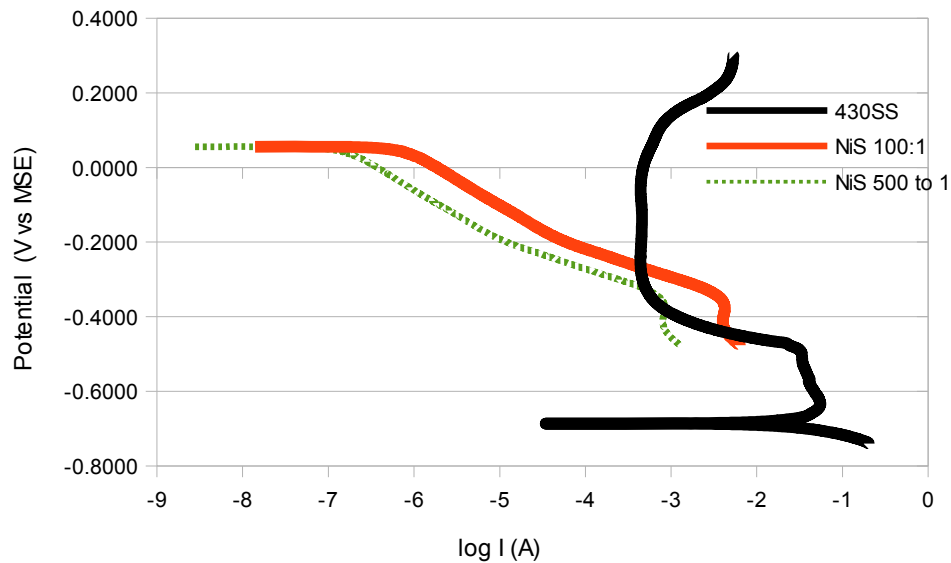


Figure 31: Surface area ratios needed to maintain passivate Type 430 at room temperature

### Transpassivation

The OCP and corrosion potentials of the cathode materials would also indicate whether transpassivation could occur in a GCAP systems. If the OCP or corrosion potential is greater than the potential above which transpassivation

occurs in the stainless steel, then the protective oxide film could be removed and corrosion of the stainless steel would be accelerated. From Figure 28., one can see the the passive region of the Type 430 stainless steel at room temperature is approximately from  $-0.4 V_{MSE}$  to  $0.1 V_{MSE}$ . Both the NiS,  $0.05 V_{MSE}$ , and NiS(Ni),  $-0.15 V_{MSE}$ , potentials fall within this range. Similarly observations were made at  $60^{\circ}\text{C}$ , and can be observed in Figure 29, and thus there would be no issue of transpassivation in a GCAP system that used either material at room temperature or  $60^{\circ}\text{C}$ .

### **Overall Circuit Resistance**

Lastly, observations from the galvanic couple experiments indicate that NiS(Ni) does contribute greatly to the overall circuit resistance when coupled to the Type 430 array in 93.5 wt%  $\text{H}_2\text{SO}_4$  at room temperature. No shielding effects were observed as there was very little variance in the potentials on the surface of the stainless steel coupons along the three rows of the array. This result was expected since the throwing power of such a GCAP system is only limited by the overall circuit resistance of the system. In this system, the anode and cathode have high conductivity and thus would unlikely be the source of the circuit resistance. The electrolyte,  $\text{H}_2\text{SO}_4$ , also possesses good conductivity and does not contribute greatly to the overall circuit resistance.

## Summary

NiS and NiS(Ni) electrodes are able to generate the  $I_{crit}$  needed to passivate and maintain the passivity of the stainless steel in such a galvanic couple anodic protection system in a 1:1 anode/cathode surface area ratio. A anode/cathode surface area of 10:1 is able to passivate Type 430 stainless steel while a ratio of 100:1 is able to maintain passivity. NiS corrodes when exposed to concentrated  $H_2SO_4$ , however, its corrosion rate is relatively low. Therefore, systems could be designed such that the corrosion of the cathode is taken into consideration when determining the lifetime of a NiS cathode. Transpassivation is not an issue when using NiS or NiS(Ni) electrodes. NiS has a high electric conductivity and does not contribute greatly to the overall circuit resistance.

Type 430-NiS GCAP systems are not practical in an industrial setting, due to the large anode/cathode surface area ratio (20:1) needed to passivate the stainless steel, NiS could be used to protect nickel-containing austenitic stainless steels. Stainless steels such as Type 304 and 316, which are already widely used in sulphuric acid manufacturing, have been shown to undergo periodic oscillations. Kish [9] has shown that anodic polarization behaviour is Type 304L is similar to that of Type 430 in concentrated sulphuric acid, shown in Figure 32. Nakahara et al. [49] has shown that GCAP systems using Pt and Au have been able to cease the process fluctuations associated with using Type 316 and thus reducing the

overall corrosion rate of the systems. NiS has shown to maintain passivity of Type 430 using anode/cathode surface area ratio of 100:1, which is on par with surface area ratios used by Nakahara et al. in industrial settings. Thus NiS cathodes of much smaller size could be used to maintain passivity in systems which use nickel containing austenitic stainless steels.

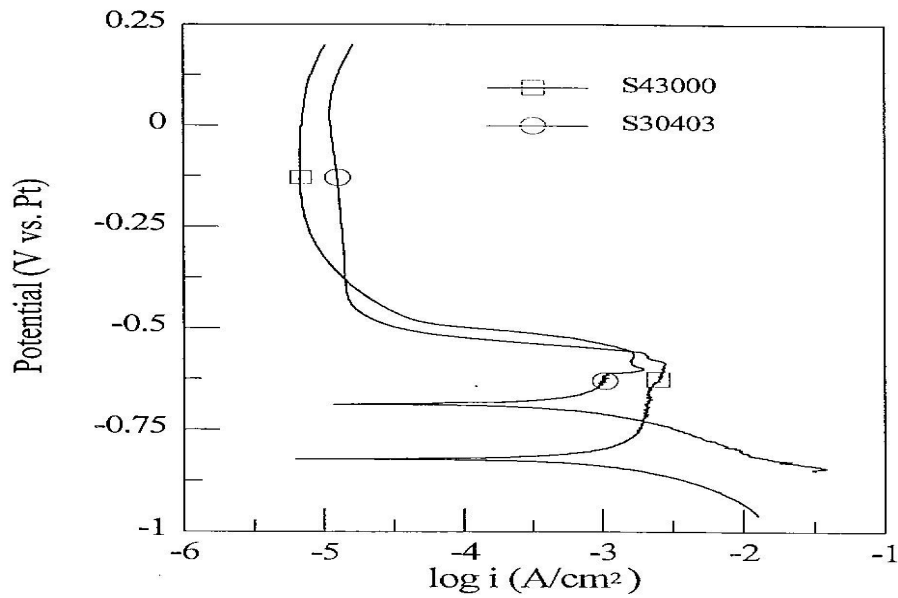


Figure 32: Comparison of anodic polarization behaviour of Type 430 and Type 304L in 93.5 wt%  $H_2SO_4$  at 60 °C [9]

## **CHAPTER 6**

### **Conclusion and Future work**

The objective of this study was to develop a better understanding of the behaviour of NiS galvanically coupled to non-Ni containing stainless steels to determine whether it can be used in a GCAP system. A comprehensive review of the relevant literature was conducted. Ni containing austenitic stainless steels have been found to exhibit spontaneous periodic active – passive potential oscillations when exposed to concentrated  $H_2SO_4$ . The cause of the oscillations observed was the production of an intermediate corrosion product formed during active corrosion. The formation and dissolution of the NiS corrosion product is essential for the active – passive corrosion potential oscillations seen in the Ni containing

stainless steels.

While effective at controlling corrosion in  $H_2SO_4$  manufacturing, ICAP systems were shown to have a number of issues. GCAP systems have not been widely utilized, but offered some solutions to these issues. GCAP systems have been developed using Pt and Au as the cathode materials. More inexpensive cathode materials such as PANI have been used but are much less effective. The ability of metal sulphides such as NiS, to form galvanic couples has been shown, thus suggesting the such metal sulphides could be used in GCAP systems.

Experiments were conducted to investigate the differences in electrochemical behaviour between monolithic NiS and NiS(Ni); and to compare their behaviour to the Pt cathode material already used in GCAP systems. The NiS and NiS(Ni) electrodes are able to provide the necessary current, up to two orders of magnitude greater than the  $i_{crit}$  needed for passivation, to passivate Type 430 stainless steel, in a 1:1 surface area ratio, room temperature and 60 °C. In comparison to Pt, these electrodes are able to provide current densities one order of magnitude greater than Pt at both temperatures at the passivation potential,  $E_{pp}$ , of the Type 430 stainless steel. The appropriate anode (stainless steel) to cathode (NiS) ratios that will protect the Type 430 stainless steel were determined. NiS and NiS(Ni) electrodes are able to provide the  $I_{crit}$  needed to passivate Type 430 at anode/cathode ratios of 10:1, while NiS(Ni) electrodes were able to provide the

$I_{crit}$  needed to passivate the Type 430 stainless steel at a ratio of 20:1. In addition it was shown that the NiS(Ni) electrode was able to maintain passivity of the Type 430 stainless steel array using a surface area ratio of 100:1.

NiS was shown not to be inert in concentrated  $H_2SO_4$  and an estimated corrosion rate was calculated via Tafel extrapolation, 0.014 mm/yr at room temperature and 0.128 mm/yr at 60 °C. In addition, the corrosion potential of NiS type electrodes is lower than that of the transpassivation potential of Type 430 stainless steel and thus transpassivation can be eliminated as an issue in Type 430 – NiS GCAP systems. NiS is relatively stable in concentrated  $H_2SO_4$  and GCAP systems that employ monolithic NiS have the ability to maintain the integrity of such systems for an extended period of time, if they are designed properly. Work needs to be conducted on such steels as well as long term exposures of monolithic NiS need to be conducted, as the issue of fouling of cathodes was not studied in this project. In addition, weight loss measurements need to be conducted on monolithic NiS to determine its corrosion rate.

## References

- [1] Davies, Michael. *Materials Selection for Sulfuric Acid*. N.p.: Materials Technology Institute, 2005. Print.
- [2] Louie, Douglas K. *Handbook of Sulphuric Acid Manufacturing*. Thornhill, Ont.: DKL Engineering 2005. Print.
- [3] International Nickel Company, *The Corrosion Resistance of Nickel Containing Alloys in Sulfuric Acid and Related Compounds*. 1983. Print.
- [4] Riggs, Olen L., Carl E. Locke, and Norman E. Hamner. *Anodic Protection: Theory and Practice in the Prevention of Corrosion*. New York: Plenum, 1981. Print.
- [5] Roberge, Pierre R. *Handbook of Corrosion Engineering*. New York: McGraw-Hill, 2000. Print.
- [6] Z.A. Foroulis, I & EC Process Design and Development, **4**, 23 (1965).
- [7] J.R. Rodda, M.B. Ives, J.R. Kish, *Materials Performance*, **44**, 7 (2005).
- [8] J.R. Rodda, M.B. Ives, J.R. Kish, *Materials Performance*, **44**, 8 (2005).
- [9] Kish, Joseph R. *Active - Passive Corrosion of Fe-Cr-Ni Alloys in Hot Concentrated Sulfuric Acid Solution*. Thesis. McMaster University, 1999. Print.
- [10] Li, Yanxu. *Corrosion of Nickel-containing Stainless Steel in Concentrated Sulphuric Acid*. Thesis. McMaster University. 2006. Print
- [11] H.H. Uhlig. *Corrosion and Corrosion Control*, 2<sup>nd</sup> ed., John Wiley & Sons, Inc., New York, 1971.
- [12] C. Wagner and W. Traud, *Z. Elektrochem.*, **44**, 391 (1938).
- [13] M. Stern and A.L. Geary, *J. Electrochem. Soc.*, **104**, 56 (1957).
- [14] J. Keir, *Phil. Trans. Royal. Soc.*, **80**, 359 (1790)

- [15] A. J. Davenport, L.J. Oblonsky, M.P. Ryan and M.F. Toney, *J. Electrochem. Soc.*, **147**, 6 (2000).
- [16] M. Cohen, in *Passivity of Metals* (eds. R.P. Frankenthal and J. Kruger), p. 521. *Electrochem. Soc.*, Princeton, N.J. (1978)
- [17] B.D. Cahan and C.T. Chen, *J. Electrochem. Soc.*, **129**, 921 (1982).
- [18] J. Kruger, *Corros. Sci.*, **29**, 2 (1989)
- [19] N.E. Hakiki, S. Boudin, B. Rondot and M.Da. Cunha Belo, *Corr. Sci.*, **27**, 11 (1995).
- [20] C.O.A Olsson, D. Landolt. *Electrochim. Acta.*, **48** (2003).
- [21] B. Elsener, A. Rossi, *Material Science Forum.*, **192**, 225 (1995).
- [22] V.S. Rao, L.K. Singhal, *J. Mater. Sci.*, **44**, 2327 (2009).
- [23] W. Y. Lai, W. Z. Zhao, Z. F. Yin and J. Zhang, *Surf. Interface Anal.*, **44**, 418 (2012).
- [24] B. Mazurkiewicz, *Electrochim. Acta*, **38**, 495 (1993).
- [25] J. Banaś, B. Mazurkiewicz, B. Stypula, *Eletrochim. Acta*, **37**, 1069 (1992).
- [26] J.R. Kish, M.B. Ives, J.R. Rodda, *Corros, Sci.*, **45**, 1571 (2003).
- [27] R.M. Kain and P.E. Morris, “Anodic Protection of Fe-Cr-Ni-Mo Alloys in Concentrated Sulphuric Acid”, Paper No. 149, CORROSION 76, NACE, Houston (1976)
- [28] Y.S. Chang, “Active Passive Corrosion Behaviour”, PhD Thesis, University of Cambridge (1984).
- [29] R. Matsushashi, H.Abo, S. Abe and H. Kihira, *Corros. Eng.*, **36**, 531 (1987)
- [30] R.J. Gillespie and E.A. Robinson, “Sulfuric Acid in Non-Aqueous Solvent Systems”, T.C. Waddington (ed.), 117, *Acedemic Press*, New York (1965).

- [31] P.W. Atkins, Physical Chemistry, W.H. Freeman and Co., New York (1986).
- [32] J.E. Roughton, J. Appl. Chem., I. Suppl., **2**, 141 (1951).
- [33] R.H. Rhodes and C.B. Barbour, Ind. Eng. Chem., **15**, 850 (1923)
- [34] C.M. Gable, H.F. Betz and S.H. Maron, J. Amer. Chem. Soc., **72**, 1445 (1950)
- [35] M. Liler, Reaction Mechanisms in Sulphuric Acid, Academic Press Inc., New York (1971).
- [36] E. Högfeltdt, Acta Cientif. Venezolana, **17**, 13 (1966).
- [37] N. Sridhar, “Mechanism of Corrosion in Concentrated Sulfuric Acid”, in Proceedings SULHPUR 85, The British Sulphur Corporation Ltd., London (1985).
- [38] B. Stypula and J. Banaś, Electrochem. Acta, **38**, 2309 (1993).
- [39] F. Beck, Electrochim., **27**, 442 (1972).
- [40] H. Hoffman, Z. Elektrochem., **27**, 442 (1921)
- [41] A.J. Arvía and J.S.W. Carrozza, Electrochim. Acta, **11**, 1641, (1966)
- [42] H.A. Garrera, J.W.S. Carrozza and A.J. Arvía, Electrochim. Acta, **13**, 771, (1968)
- [43] J.W.S. Carrozza, H.A. Garrera and A.J. Arvía, Electrochim. Acta, **14**, 205, (1969)
- [44] A.J. Arvía, H.A. Garrera and J.W.S. Carrozza, Electrochim. Acta, **16**, 79, (1971)
- [45] C. Edeleanu, Anti-Corrosion Methods and Materials, **2,7**, (1955)
- [46] J.I. Munro and W.W. Shim, Materials Performance, 13104 (2001).

- [47] Jones, Denny A. *Principles and Prevention of Corrosion*. Upper Saddle River, NJ: Prentice Hall, 1996. Print.
- [48] G.Bianchi, A. Barosi, and S. Trasatti, *Electrochim. Acta*, **10**, 83 (1965).
- [49] M. Nakahara, J. Takahashi and N. Nakatani, *Corros. Eng.*, **51**, 133 (2002).
- [50] L. Zhong, S. Xiao, J. Hu, H. Zhu, F. Gan, *Corros. Sci.*, **48**, 3960 (2006).
- [51] "Inorganic Crystal Structure Database." *Inorganic Crystal Structure Database*. FIZ Karlsruhe, n.d. Web.
- [52] L. Zhou, H. Li, L. Xu, *Chinese J. of Geochem.*, **25**, 230 (2006).
- [53] C. Pearce, R. Patrick, D. Vaughan, *Reviews in Mineralogy and Geochemistry*, **61**, 127 (2006)
- [54] S.R.Krishnakumar, N.Shanthi, D.D.Sarma, *Physical Review B*, 66 (2002).
- [55] S.R. Rao and J.A. Finch, *Canadian Metallurgical Quarterly*, **27**, 253 (1988)
- [56] P.R. Holmes and F. K. Crundwell, *Hydrometallurgy*, **39**, 353 (1995)
- [57] C.C. Sui, S.H.R. Brienne, S.R. Rao, Z. Xu and J.A. Finch, *Minerals Engineering*, **8**, 1523 (1995)
- [58] R. Cruz, R.M. Luna Sanchez, G.T. Lapidus. I. Gonzalez, M. Monroy, *Hydrometallurgy*, **78**, 198 (2005)
- [59] S.M.J. Koleini, V. Aghazadeh, Ake Sandstrom, *Minerals Engineering*, **24**, 381 (2011)
- [60] A.P. Metha, L.E. Murr, *Hydrometallurgy*, **9**, 235 (1983)
- [61] A.Pal, J.R. Kish, S. Jones. K. Coley, Unpublished data, McMaster University
- [62] W. Fredriksson, S. Malmgren, T. Gustafsson, M. Gorgoi, K. Edström, *Appl. Surf. Sci.*, **258**, 5790 (2012).

M.ASc. Thesis – A. Pal; McMaster University – Materials Engineering

[63] F. Zucchi, G. Gilli, P. A. Borea and G. Trabanelli, *Corros. Sci.*, **12**, 699 (1972).